9 Mott transition: DFT+U vs DFT+DMFT

Eva Pavarini
Institute for Advanced Simulation
Forschungszentrum Jülich

Contents

E. Pavarini, E. Koch, R. Scalettar, and R. Martin (eds.)
The Physics of Correlated Insulators, Metals, and Superconductors
Modeling and Simulation Vol. 7
Forschungszentrum Jülich, 2017, ISBN 978-3-95806-224-5
http://www.cond-mat.de/events/correl17

1 Introduction

One of the early successes of quantum mechanics was explaining the difference between metals and insulators. The core of this theory is the *independent-electron picture*. In the latter, the electronic states of a given periodic system, a crystal, are described via a set of bands filled following the Pauli principle. As a result, two cases are possible: in the first, each band is either completely filled or totally empty (*band insulator*), and in the second, some of the bands are only partially filled (*conventional metal*). In a system in which all bands are either full or empty, a finite energy is required to bring one electron from the ground state to the lowest-lying excited state. Indeed, an insulator can be viewed as a system with an *energy gap* in the excitation spectrum. The energy gap is not uniquely defined, since it has a different nature depending on the experimental tool used to measure it. Photoemission and inverse photoemission probe the spectral function. The latter yields the charge gap

$$E^c_{\rm gap} = E_0(N+1) + E_0(N-1) - 2E_0(N),$$

where $E_0(N)$ is the ground-state energy for N electrons. This is the difference between the ionization energy, $I = E_0(N-1) - E_0(N)$ and electronic affinity, $A = E_0(N) - E_0(N+1)$. In the independent-electron picture, at $T = 0$

$$E_0(N) = 2\sum_{m\boldsymbol{k}} \varepsilon_{m\boldsymbol{k}}\, \Theta(-\varepsilon_{m\boldsymbol{k}} + \varepsilon_F),$$

where m is an index labelling different bands, $\varepsilon_{m\mathbf{k}}$ the band dispersion, ε_F the Fermi level and $\Theta(x)$ the Heaviside step function. Thus the charge gap is basically identical to the difference

$$E^o_{\rm gap} = E_1(N) - E_0(N).$$

where $E_1(N)$ is the energy of the N-electron first excited state (Fig. 1). The energy difference $E^o_{\rm gap}$ can be directly probed in experiments which do not change the number of electrons, e.g., absorption spectroscopy. In the presence of a gap, the finite-temperature properties are typically characterized by an activation energy ΔE. For example, the static optical conductivity of a band insulator has, in first approximation, the low-temperature form

$$\sigma(T) \sim \sigma_0(T) e^{-\Delta E/2k_BT},$$

where ΔE is the band gap and $\sigma_0(T)$ a prefactor. The size of the gap varies from system to system, giving rise to different behaviors and appearances. Representative examples of band insulators are two well known materials with the same crystal structure and yet rather different properties, diamond and silicon. Diamond is transparent thanks to its large gap ($\sim$ 5.5 eV). Silicon has a smaller gap ($\sim$ 1.1 eV), a gray color and could be taken at a first glance for a metal. A conventional metal behaves very differently than a band insulator, however. In a conventional metal, since some bands are partially empty, it is possible to excite electrons with infinitesimal energy. Thus, e.g., the conductivity is finite even at $T = 0$

$$\sigma(0) \sim \frac{ne^2\tau}{m_e},$$

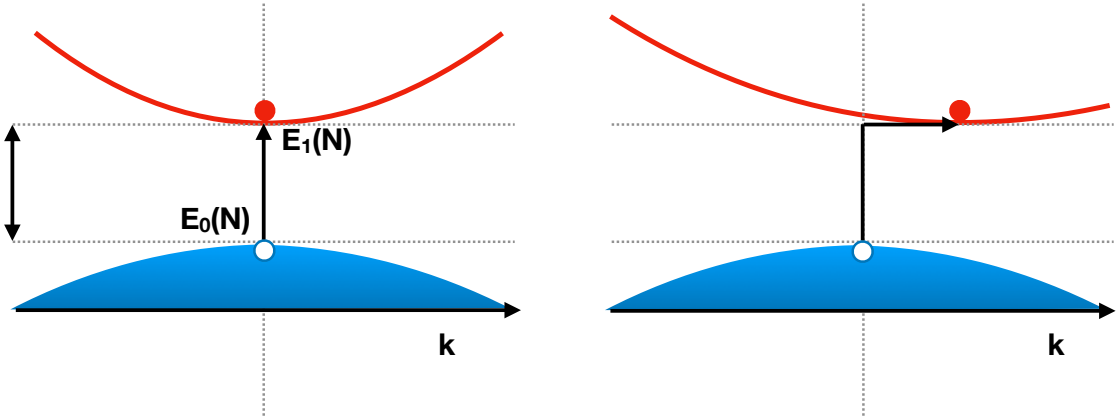

Fig. 1: *The band gap $E_g^o = E_1(N) - E_0(N)$ in the independent-electron picture. Left: direct gap. Right: indirect gap. Silicon and diamond both have an indirect gap. Blue: top of the filled valence band. Red: bottom of the empty conduction band.*

where n is the electron density and τ the average time between two collisions. Classical examples of conventional metals are gold, silver, and copper. They are all characterized by shiny metallic colors. Have we then explained all matter via the rather simple independent-electron band theory? One could naively think that this is, indeed, the case. Reality, however, has always surprises in store. It became clear early on that the independent-electron theory is not the complete story. Some transition-metal oxides, which were supposed to be good metals in the independent-electron picture, turned out to be either insulators or very bad conductors. It was soon understood that a possible cause of the anomalous behavior could be the electron-electron Coulomb repulsion; the latter could localize electrons giving rise to a metal-insulator transition (MIT). That things are very different when the electronic Coulomb interaction is taken into account can be seen already in Fig. 2, which shows the charge gap for an idealized atom made by a single level $\varepsilon_d < 0$ occupied by one electron. If we assume that the electrons do not interact ($U = 0$), the charge gap is zero

$$E_{\rm gap}^c = [E_0(2) - E_0(1)] + [E_0(0) - E_0(1)] = \varepsilon_d - \varepsilon_d = 0.$$

If, however, electrons repel each other ($U \neq 0$), the gap is finite

$$E_{\rm gap}^c = U.$$

Let us define *strongly-correlated systems* the materials whose behavior qualitatively differs from the independent-electron picture because of the electron-electron repulsion. While the theory of conventional metals and band insulators is rather straightforward, the theory of the MIT in strongly-correlated systems has kept theoreticians busy for almost a century, and still the problem is only partially solved. This happens because, when the independent-electron picture fails, we are confronted with the hardness of the quantum many-body problem. The latter can already be grasped by looking at the classical N body problem (Fig. 3), describing masses interacting via gravity. When only one body is present, there is no interaction, and the problem

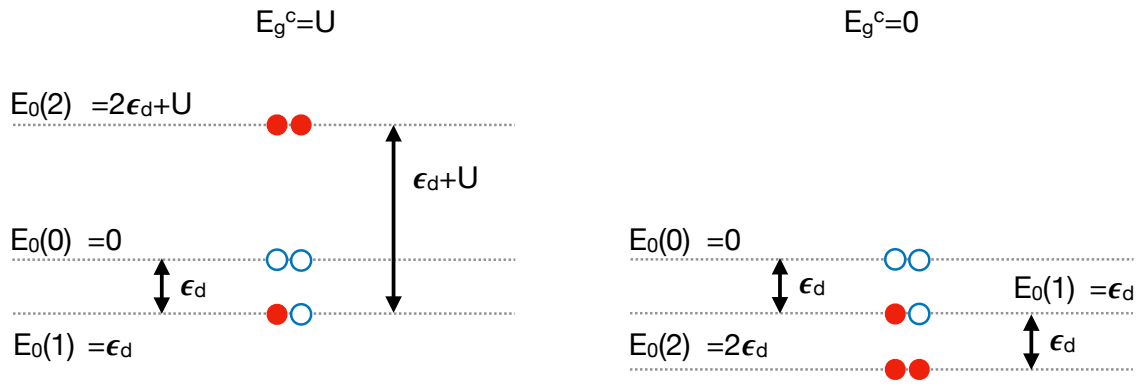

Fig. 2: *The charge gap for an idealized atom described by a level $\varepsilon_d < 0$ occupied by one electron ($N = 1$). Left: When two electrons are on the same level, the system has energy $2\varepsilon_d + U$, where U is the electron-electron repulsion. Right: Non-interacting-electron picture.*

is trivial. For two bodies we can find the analytical solution by working in the center of mass and relative coordinates system. The general three-body problem is a major challenge [1] and it can lead to chaotic behavior; the complexity of the N-body problem grows dramatically with the number of bodies involved [2]. Quantum effects further add to the complications, and the exact solution of the many-body problem is totally out of reach. Even if we cannot count on the exact diagonalization of the full many-body Hamiltonian, however, this does not imply the end of physics. We can still explain the origin of specific co-operative behaviors, such as the nature of the insulating or metallic state; we need, however, to first identify the core nature of the phenomenon along with the relevant effective entities involved, and then build the corresponding effective theory. A natural question arises at this point. Although we know that it eventually fails for strongly-correlated systems, the independent-electron picture is very appealing for its simplicity. Furthermore it works rather well for many systems, at least in first approximation; we have already mentioned among insulators silicon and diamond, and among metals gold, silver or copper. Could we then perhaps explain strongly-correlated insulators without leaving the independent-electron picture, via, e.g, a Coulomb-induced one-electron potential of some type? Or do we really need a more complex theory, in which true many-body effects – those that cannot be reduced to a simple potential – are key? Let us call a system for which the first picture applies *Slater insulator* and one for which the second picture is relevant *Mott insulator*. The answer to the question above is important also in view of the fact that, while solving exactly the many-body problem is basically impossible, we do have very advanced tools to solve material-specific one-electron-like Hamiltonians. These are *ab-initio* methods based on density-functional theory (DFT) in the local-density approximation or its simple extensions. Is it possible to find a *simple* potential that captures the essential nature of the MIT and can be easily embedded in DFT-based codes? The DFT+U method [3] is one of the most important attempts in this direction; in this approach Coulomb repulsion effects are treated at the *static mean-field* level and they are then essentially reduced to a spin-, site- and orbital-

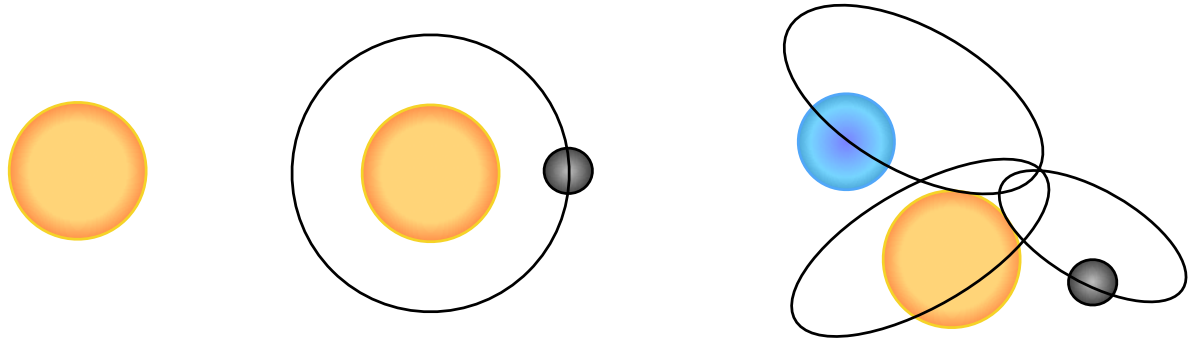

Fig. 3: *The increasing complexity of the classical N-body problem. One body: no interaction. Two bodies: we can find the solution analytically. Shown is a solution describing a lighter body rotating about a heavier body. Three-body: chaotic solutions are possible.*

dependent potential. The resulting MIT is of the Slater type, and it occurs at the onset of long-range magnetic order. Unfortunately, correlated insulators typically do not behave in this way, however. Although most of them have a magnetic ground state, above the magnetic transition temperature T_N they usually remain insulators; furthermore, they typically behave as local-moment paramagnets with Curie-Weiss magnetic susceptibilities. Instead, in the non-magnetic phase DFT+U yields metallic Pauli-like paramagnets. This shows that some crucial aspects are missing in DFT+U. Which ones, however? To answer to this question, one can use an alternative approach. This consist in giving up the band picture and DFT completely, switch to simple representative models and try to solve them beyond the static mean-field level via many-body techniques. Even in simple models, however, truly strongly-correlated phenomena, which escape a static mean-field description, remain a challenge. An example is the Kondo effect, which was solved only after decades of struggle, and the solution lead to the developments of new theoretical approaches such as the numerical renormalization group. In the case of the metal-insulator transition, the breakthrough was the *dynamical mean-field theory* (DMFT) [4–8]. This method was at first designed to solve the one-band *Hubbard model*. It consists in mapping the lattice Hubbard model into a self-consistent quantum-impurity model, described for example by the *Anderson Hamiltonian*. The DMFT technique succeeds in describing the Coulomb-driven transition from paramagnetic metal to local-moment paramagnetic insulator. Furthermore, it can be used for solving material-specific Hubbard models built from DFT-based calculations; this is the DFT+DMFT approach. In this lecture, after an introduction to the Hubbard and the Anderson Hamiltonian, we will discuss some of the basic ideas behind both the DFT+U and the DFT+DMFT method. We will compare the very different pictures of the metal-insulator transition emerging from the two approaches, the first of the Slater and the second of the Mott type. As a concluding remark, it is important to remember that band, Slater, and Mott insulators do not exhaust all possible types of insulators. Electron localization can, e.g., also occur because of disorder alone. This phenomenon is known as Anderson localization [9]. Although the latter is a very important and interesting effect, we will not discuss it in this lecture.

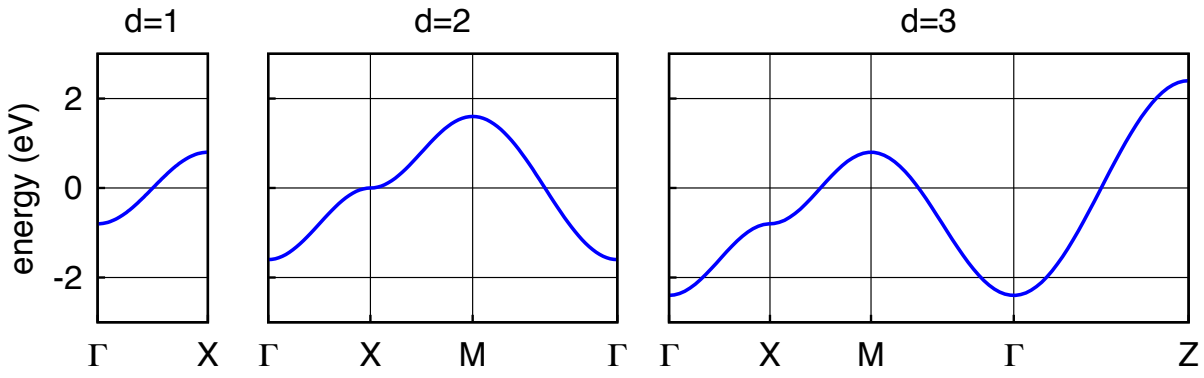

Fig. 4: *Band structure of the one-band tight-binding model (hypercubic lattice). The hopping integral is* $t = 0.4$ *eV. From left to right: one-, two-, and three-dimensional case. At half filling* ($n = 1$) *the Fermi level is at zero energy. The* $\boldsymbol{k}$ *points are* $\Gamma = (0,0,0)$, $X = (\pi/a, 0, 0)$, $M = (\pi/a, \pi/a, 0)$, *and* $Z = (0, 0, \pi/a)$.

2 The Hubbard model

2.1 Introduction

The simplest lattice model describing a correlated system is the one-band Hubbard model

$$\hat{H} = \underbrace{\varepsilon_d \sum_i \sum_\sigma c^\dagger_{i\sigma} c_{i\sigma}}_{\hat{H}_d} \underbrace{-t \sum_{\langle ii' \rangle} \sum_\sigma c^\dagger_{i\sigma} c_{i'\sigma}}_{\hat{H}_T} + \underbrace{U \sum_i \hat{n}_{i\uparrow} \hat{n}_{i\downarrow}}_{\hat{H}_U} = \hat{H}_d + \hat{H}_T + \hat{H}_U, \qquad (1)$$

where ε_d is the on-site energy, t is the hopping integral between first-nearest neighbors $\langle ii' \rangle$, and U the on-site Coulomb repulsion; $c^\dagger_{i\sigma}$ creates an electron in a Wannier state with spin σ centered at site i, and $\hat{n}_{i\sigma} = c^\dagger_{i\sigma} c_{i\sigma}$.

In the $U = 0$ limit the Hubbard model describes a system of independent electrons. The Hamiltonian is then diagonal in the Bloch basis

$$\hat{H}_d + \hat{H}_T = \sum_{\boldsymbol{k}\sigma} \Big[\varepsilon_d + \varepsilon_{\boldsymbol{k}} \Big] c^\dagger_{\boldsymbol{k}\sigma} c_{\boldsymbol{k}\sigma}.$$

The energy dispersion $\varepsilon_{\boldsymbol{k}}$ depends on the geometry and dimensionality d of the lattice. For a hypercubic lattice of dimension d

$$\varepsilon_{\boldsymbol{k}} = -2t \sum_{\nu=1}^{d} \cos(k_{r_\nu} a),$$

where a is the lattice constant, and $r_1 = x, r_2 = y, r_3 = z$. The energy $\varepsilon_{\boldsymbol{k}}$ does not depend on the spin. In Fig. 4 we show $\varepsilon_{\boldsymbol{k}}$ in the one-, two- and three-dimensional cases. The corresponding density of states is shown in Fig. 5.

In the opposite limit ($t = 0$) the Hubbard model describes a collection of isolated atoms. Each

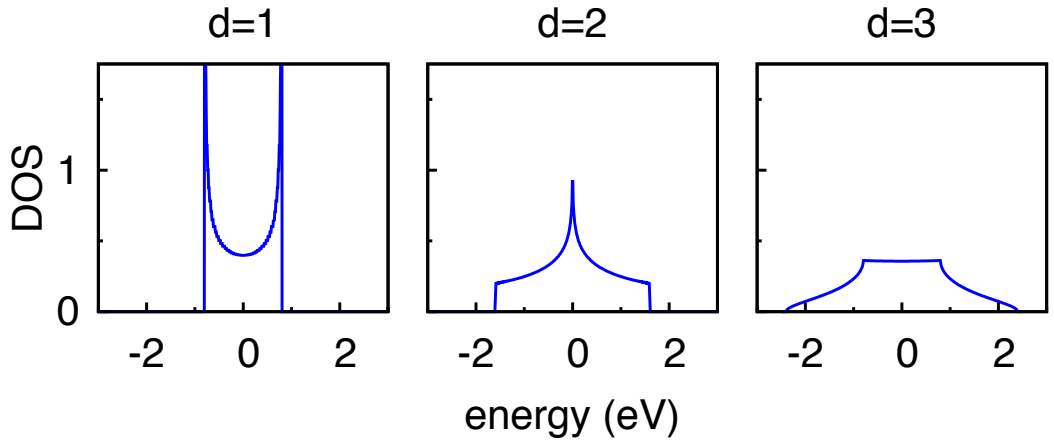

Fig. 5: *Density of states (DOS) per spin, $\rho(\varepsilon)/2$, for a hypercubic lattice in one, two, and three dimensions. The energy dispersion is calculated for $t = 0.4$ eV. The curves exhibit different types of Van-Hove singularities.*

atom has four electronic many-body states

$\|N, S, S_z\rangle$			N	S	$E(N)$
$\|0, 0, 0\rangle$	$=$	$\|0\rangle$	0	0	0
$\|1, \frac{1}{2}, \uparrow\rangle$	$=$	$c^\dagger_{i\uparrow}\|0\rangle$	1	1/2	ε_d
$\|1, \frac{1}{2}, \downarrow\rangle$	$=$	$c^\dagger_{i\downarrow}\|0\rangle$	1	1/2	ε_d
$\|2, 0, 0\rangle$	$=$	$c^\dagger_{i\uparrow}c^\dagger_{i\downarrow}\|0\rangle$	2	0	$2\varepsilon_d + U$

where $E(N)$ is the total energy, N the total number of electrons and S the total spin. We can express the atomic Hamiltonian $\hat{H}_d + \hat{H}_U$ in a form in which the dependence on $\hat{N}_i$, $\hat{S}_i$, and $\hat{S}^i_z$ is explicitly given

$$\hat{H}_d + \hat{H}_U = \varepsilon_d \sum_i \hat{n}_i + U \sum_i \left[-\left(\hat{S}^i_z\right)^2 + \frac{\hat{n}^2_i}{4} \right],$$

where $\hat{S}^i_z = (\hat{n}_{i\uparrow} - \hat{n}_{i\downarrow})/2$ is the z component of the spin operator and $\hat{n}_i = \sum_\sigma \hat{n}_{i\sigma} = \hat{N}_i$.
In the large t/U limit and at half filling we can downfold charge fluctuations and map the Hubbard model into an effective spin model of the form

$$\hat{H}_S = \frac{1}{2} \Gamma \sum_{\langle ii' \rangle} \left[\boldsymbol{S}_i \cdot \boldsymbol{S}_{i'} - \frac{1}{4} \hat{n}_i \hat{n}_{i'} \right]. \tag{2}$$

The coupling Γ can be calculated by using second-order perturbation theory. For a state in which two neighbors have opposite spin, $|\uparrow, \downarrow\rangle = c^\dagger_{i\uparrow} c^\dagger_{i'\downarrow} |0\rangle$, we obtain the energy gain

$$\Delta E_{\uparrow\downarrow} \sim -\sum_I \langle \uparrow, \downarrow | \hat{H}_T | I \rangle \langle I \left| \frac{1}{E(2) + E(0) - 2E(1)} \right| I \rangle \langle I | \hat{H}_T | \uparrow, \downarrow \rangle \sim -\frac{2t^2}{U}.$$

Here $|I\rangle$ ranges over the excited states with one of the two neighboring sites doubly occupied and the other empty, $|\uparrow\downarrow,0\rangle = c^\dagger_{i\uparrow}c^\dagger_{i\downarrow}|0\rangle$, or $|0,\uparrow\downarrow\rangle = c^\dagger_{i'\uparrow}c^\dagger_{i'\downarrow}|0\rangle$; these states can be occupied via virtual hopping processes. For a state in which two neighbors have parallel spins, $|\uparrow,\uparrow\rangle = c^\dagger_{i\uparrow}c^\dagger_{i'\uparrow}|0\rangle$, no virtual hopping is possible because of the Pauli principle, and $\Delta E_{\uparrow\uparrow} = 0$. Thus

$$\frac{1}{2}\Gamma \sim (\Delta E_{\uparrow\uparrow} - \Delta E_{\uparrow\downarrow}) = \frac{1}{2}\frac{4t^2}{U}. \tag{3}$$

The exchange coupling $\Gamma = 4t^2/U$ is positive, i.e., antiferromagnetic.
Canonical transformations [10] provide a scheme for deriving the effective spin model systematically at any perturbation order. Let us consider a unitary transformation of the Hamiltonian

$$\hat{H}_S = e^{i\hat{S}}\hat{H}e^{-i\hat{S}} = \hat{H} + \Big[i\hat{S},\hat{H}\Big] + \frac{1}{2}\Big[i\hat{S},\Big[i\hat{S},\hat{H}\Big]\Big] + \dots.$$

We search for a transformation operator that eliminates, at a given order, hopping integrals between states with a different number of doubly-occupied states. To do this, first we split the kinetic term $\hat{H}_T$ into a component $\hat{H}^0_T$ that does not change the number of doubly-occupied states and two terms that either increase it ($\hat{H}^+_T$) or decrease it ($\hat{H}^-_T$) by one

$$\hat{H}_T = -t\sum_{\langle ii'\rangle}\sum_\sigma c^\dagger_{i\sigma}c_{i'\sigma} = \hat{H}^0_T + \hat{H}^+_T + \hat{H}^-_T,$$

where

$$\hat{H}^0_T = -t\sum_{\langle ii'\rangle}\sum_\sigma \hat{n}_{i-\sigma}\, c^\dagger_{i\sigma}c_{i'\sigma}\, \hat{n}_{i'-\sigma} - t\sum_{\langle ii'\rangle}\sum_\sigma \Big[1-\hat{n}_{i-\sigma}\Big]c^\dagger_{i\sigma}c_{i'\sigma}\Big[1-\hat{n}_{i'-\sigma}\Big],$$

$$\hat{H}^+_T = -t\sum_{\langle ii'\rangle}\sum_\sigma \hat{n}_{i-\sigma}\, c^\dagger_{i\sigma}c_{i'\sigma}\Big[1-\hat{n}_{i'-\sigma}\Big],$$

$$\hat{H}^-_T = \Big(\hat{H}^+_T\Big)^\dagger.$$

The term $\hat{H}^0_T$ commutes with $\hat{H}_U$. The remaining two terms fulfill the commutation rules

$$[\hat{H}^\pm_T, \hat{H}_U] = \mp U\hat{H}^\pm_T.$$

The operator $\hat{S}$ can be expressed as a linear combination of powers of the three operators $\hat{H}^0_T, \hat{H}^+_T$, and $\hat{H}^-_T$. The actual combination, which gives the effective spin model at a given order, can be found via a recursive procedure [10]. At half filling and second order, however, we can simply guess the form of $\hat{S}$ that leads to the Hamiltonian (2). By defining

$$\hat{S} = -\frac{i}{U}\Big(\hat{H}^+_T - \hat{H}^-_T\Big)$$

we obtain

$$\hat{H}_S = \hat{H}_U + \hat{H}^0_T + \frac{1}{U}\Big(\Big[\hat{H}^+_T,\hat{H}^-_T\Big] + \Big[\hat{H}^0_T,\hat{H}^-_T\Big] + \Big[\hat{H}^+_T,\hat{H}^0_T\Big]\Big) + \mathcal{O}(U^{-2}).$$

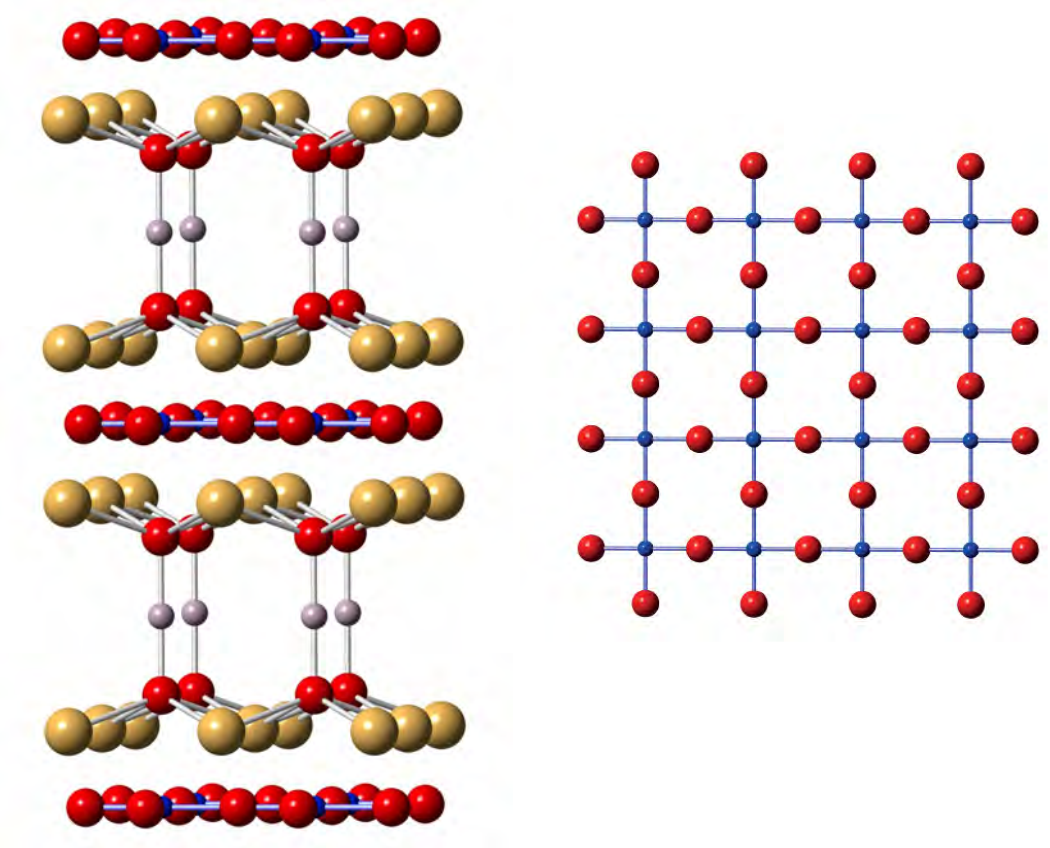

Fig. 6: *Left: Crystal structure of $HgBa_2CuO_4$ showing the two-dimensional CuO_2 layers. Spheres represent atoms of Cu (blue), O (red), Ba (yellow), and Hg (grey). Right: A CuO_2 layer. The hopping integral t between neighboring Cu sites is $t \sim 4t_{pd}^2/\Delta_{dp}$, where t_{pd} is the hopping between Cu d and O p states and $\Delta_{dp} = \varepsilon_d - \varepsilon_p$ their charge-transfer energy.*

If we restrict the Hilbert space of $\hat{H}_S$ to the subspace with one electron per site (half filling), no hopping is possible without increasing the number of doubly-occupied states; hence, only the term $\hat{H}_T^- \hat{H}_T^+$ contributes. After some algebra, we obtain $\hat{H}_S = \hat{H}_S^{(2)} + \mathcal{O}(U^{-2})$ with

$$\hat{H}_S^{(2)} = \frac{1}{2}\frac{4t^2}{U}\sum_{ii'}\left[\boldsymbol{S}_i \cdot \boldsymbol{S}_{i'} - \frac{1}{4}\hat{n}_i\hat{n}_{i'}\right].$$

The Hubbard model (1) is rarely realized in nature in this form. To understand real materials one typically has to take into account orbital degrees of freedom, long-range hopping integrals, and sometimes longer-range Coulomb interactions or perhaps even more complex many-body terms. Nevertheless, there are very interesting systems whose low-energy properties are, to first approximation, described by (1). These are strongly-correlated organic crystals [11] (one-dimensional case) and high-temperature superconducting cuprates [12], in short HTSCs (two-dimensional case). An example of HTSC is $HgBa_2CuO_4$, whose structure is shown in Fig. 6. It is made of CuO_2 planes well divided by BaO-Hg-BaO blocks. The x^2-y^2-like states stemming from the CuO_2 planes can be described via a one-band Hubbard model. The presence of a x^2-y^2-like band at the Fermi level is a common feature of all HTSCs.

2.2 The Hubbard dimer

The Hubbard model cannot be solved exactly. It is thus interesting to consider an even simpler model, for which we can find analytically eigenvectors and eigenvalues. This is the Hubbard dimer, whose Hamiltonian is given by

$$\hat{H} = \varepsilon_d \sum_{i\sigma} n_{i\sigma} - t \sum_{\sigma} \left[c^\dagger_{1\sigma} c_{2\sigma} + c^\dagger_{2\sigma} c_{1\sigma} \right] + U \sum_{i=1,2} \hat{n}_{i\uparrow} \hat{n}_{i\downarrow}. \tag{4}$$

2.2.1 Exact diagonalization

Hamiltonian (4) commutes with the number of electron operator $\hat{N}$, the total spin $\hat{S}$ and $\hat{S}_z$. In the atomic limit, the eigenstates states can be therefore classified as

$\|N,S,S_z\rangle$			N	S	$E(N,S)$
$\|0,0,0\rangle$	$=$	$\|0\rangle$	0	0	0
$\|1,1/2,\sigma\rangle_1$	$=$	$c^\dagger_{1\sigma}\|0\rangle$	1	$1/2$	ε_d
$\|1,1/2,\sigma\rangle_2$	$=$	$c^\dagger_{2\sigma}\|0\rangle$	1	$1/2$	ε_d
$\|2,1,1\rangle$	$=$	$c^\dagger_{2\uparrow}c^\dagger_{1\uparrow}\|0\rangle$	2	1	$2\varepsilon_d$
$\|2,1,-1\rangle$	$=$	$c^\dagger_{2\downarrow}c^\dagger_{1\downarrow}\|0\rangle$	2	1	$2\varepsilon_d$
$\|2,1,0\rangle$	$=$	$\frac{1}{\sqrt{2}}\left[c^\dagger_{1\uparrow}c^\dagger_{2\downarrow} + c^\dagger_{1\downarrow}c^\dagger_{2\uparrow}\right]\|0\rangle$	2	1	$2\varepsilon_d$
$\|2,0,0\rangle_0$	$=$	$\frac{1}{\sqrt{2}}\left[c^\dagger_{1\uparrow}c^\dagger_{2\downarrow} - c^\dagger_{1\downarrow}c^\dagger_{2\uparrow}\right]\|0\rangle$	2	0	$2\varepsilon_d$
$\|2,0,0\rangle_1$	$=$	$c^\dagger_{1\uparrow}c^\dagger_{1\downarrow}\|0\rangle$	2	0	$2\varepsilon_d + U$
$\|2,0,0\rangle_2$	$=$	$c^\dagger_{2\uparrow}c^\dagger_{2\downarrow}\|0\rangle$	2	0	$2\varepsilon_d + U$
$\|3,1/2,\sigma\rangle_1$	$=$	$c^\dagger_{1\sigma}c^\dagger_{2\uparrow}c^\dagger_{2\downarrow}\|0\rangle$	3	$1/2$	$3\varepsilon_d + U$
$\|3,1/2,\sigma\rangle_2$	$=$	$c^\dagger_{2\sigma}c^\dagger_{1\uparrow}c^\dagger_{1\downarrow}\|0\rangle$	3	$1/2$	$3\varepsilon_d + U$
$\|4,0,0\rangle$	$=$	$c^\dagger_{1\uparrow}c^\dagger_{1\downarrow}c^\dagger_{2\uparrow}c^\dagger_{2\downarrow}\|0\rangle$	4	0	$4\varepsilon_d + 2U$

Let us order the $N = 1$ states as in the table above, first the spin up and then spin down block. For finite t the Hamiltonian matrix for $N = 1$ electrons takes then the form

$$\hat{H}_1 = \begin{pmatrix} \varepsilon_d & -t & 0 & 0 \\ -t & \varepsilon_d & 0 & 0 \\ 0 & 0 & \varepsilon_d & -t \\ 0 & 0 & -t & \varepsilon_d \end{pmatrix}.$$

This matrix can be easily diagonalized and yields the *bonding* $(-)$ and *antibonding* $(+)$ states

$\|1,S,S_z\rangle_\alpha$		$E_\alpha(1,S)$	$d_\alpha(1,S)$
$\|1,1/2,\sigma\rangle_+$	$= \frac{1}{\sqrt{2}}\left[\|1,1/2,\sigma\rangle_1 - \|1,1/2,\sigma\rangle_2\right]$	$\varepsilon_d + t$	2
$\|1,1/2,\sigma\rangle_-$	$= \frac{1}{\sqrt{2}}\left[\|1,1/2,\sigma\rangle_1 + \|1,1/2,\sigma\rangle_2\right]$	$\varepsilon_d - t$	2

where $d_\alpha(N)$ is the spin degeneracy of the α manifold. Let us now increase the total number of electrons. For $N = 2$ electrons (half filling), the hopping integrals only couple the three $S = 0$ states, and therefore the Hamiltonian matrix is given by

$$\hat{H}_2 = \begin{pmatrix} 2\varepsilon_d & 0 & 0 & 0 & 0 & 0 \\ 0 & 2\varepsilon_d & 0 & 0 & 0 & 0 \\ 0 & 0 & 2\varepsilon_d & 0 & 0 & 0 \\ 0 & 0 & 0 & 2\varepsilon_d & -\sqrt{2}t & -\sqrt{2}t \\ 0 & 0 & 0 & -\sqrt{2}t & 2\varepsilon_d + U & 0 \\ 0 & 0 & 0 & -\sqrt{2}t & 0 & 2\varepsilon_d + U \end{pmatrix}.$$

The eigenvalues and the corresponding (normalized) eigenvectors are

$\|2,S,S_z\rangle_\alpha$		$E_\alpha(2,S)$	$d_\alpha(2,S)$
$\|2,0,0\rangle_+$	$= a_1\|2,0,0\rangle_0 - \frac{a_2}{\sqrt{2}}\left[\|2,0,0\rangle_1 + \|2,0,0\rangle_2\right]$	$2\varepsilon_d + \frac{1}{2}\left[U + \Delta(t,U)\right]$	1
$\|2,0,0\rangle_o$	$= \frac{1}{\sqrt{2}}\left[\|2,0,0\rangle_1 - \|2,0,0\rangle_2\right]$	$2\varepsilon_d + U$	1
$\|2,1,m\rangle_o$	$= \|2,1,m\rangle$	$2\varepsilon_d$	3
$\|2,0,0\rangle_-$	$= a_2\|2,0,0\rangle_0 + \frac{a_1}{\sqrt{2}}\left[\|2,0,0\rangle_1 + \|2,0,0\rangle_2\right]$	$2\varepsilon_d + \frac{1}{2}\left[U - \Delta(t,U)\right]$	1

where

$$\Delta(t,U) = \sqrt{U^2 + 16t^2},$$

and $a_1 a_2 = 2t/\Delta(t,U)$. For $U = 0$ we have $a_1 = a_2 = 1/\sqrt{2}$, and the two states $|2,0,0\rangle_-$ and $|2,0,0\rangle_+$ become, respectively, the state with two electrons in the bonding orbital and the state with two electrons in the antibonding orbital; they have energy $E_\pm(2,0) = 2\varepsilon_d \pm 2t$; the remaining states have energy $2\varepsilon_d$ and are non-bonding. For $t > 0$, the ground state is unique and it is always the singlet $|2,0,0\rangle_-$; in the large U limit its energy is

$$E_-(2,0) \sim 2\varepsilon_d - 4t^2/U.$$

In this limit the energy difference between the first excited state, a triplet state, and the singlet ground state is thus equal to the Heisenberg antiferromagnetic coupling

$$E_o(2,1) - E_-(2,0) \sim 4t^2/U = \Gamma.$$

Finally, for $N = 3$ electrons, eigenstates and eigenvectors are

$\|3, S, S_z\rangle_\alpha$		$E_\alpha(3)$	$d_\alpha(3, S)$
$\|3, 1/2, \sigma\rangle_+$	$= \frac{1}{2}\left[\|1, 1/2, \sigma\rangle_1 + \|1, 1/2, \sigma\rangle_2\right]$	$3\varepsilon_d + U + t$	2
$\|3, 1/2, \sigma\rangle_-$	$= \frac{1}{2}\left[\|1, 1/2, \sigma\rangle_1 - \|1, 1/2, \sigma\rangle_2\right]$	$3\varepsilon_d + U - t$	2

If we exchange holes and electrons, the $N = 3$ case is identical to the $N = 1$ electron case. This is due to the particle-hole symmetry of the model.

2.2.2 Local Matsubara Green function

Let us now calculate the local Matsubara Green function for site i, defined as

$$G_{ii,\sigma}(i\nu_n) = -\int_0^\beta d\tau e^{i\nu_n\tau}\langle \mathcal{T} c_{i\sigma}(\tau) c^\dagger_{i\sigma}(0)\rangle,$$

where $\mathcal{T}$ is the time-ordering operator and ν_n a fermionic Matsubara frequency. We use to this end the Lehmann representation

$$G_{ii,\sigma}(i\nu_n) = \frac{1}{Z}\sum_{nn'N} e^{-\beta(E_n(N)-\mu N)}\left[\frac{|\langle n'N-1|c_{i\sigma}|nN\rangle|^2}{i\nu_n - [E_n(N) - E_{n'}(N-1) - \mu]}\right. \\ \left. + \frac{|\langle n'N+1|c^\dagger_{i\sigma}|nN\rangle|^2}{i\nu_n - [E_{n'}(N+1) - E_n(N) - \mu]}\right], \tag{5}$$

where $|nN\rangle$ is the N-electron eigenstate with energy $E_n(N)$, $\beta = 1/k_BT$, μ is the chemical potential, and Z the partition function. In order to calculate the Green function (5) we thus need all eigenstates and their energies; from the eigenstates we have to compute the weights $w_i^\sigma = |\langle n'N'|\hat{o}_{i\sigma}|nN\rangle|^2$, where $\hat{o}_{i\sigma}$ is either $c_{i\sigma}$ or $c^\dagger_{i\sigma}$. The Green function is by symmetry identical for spin up and spin down, and for site 1 and site 2. Thus it is sufficient to perform the calculation for $i = 1$ and $\sigma =\uparrow$. In the atomic limit, the only non-zero terms are collected in the table shown in the next page; in the first half of the table $\hat{o}_{1\uparrow} = c_{1\uparrow}$ and $N' = N$, and in the

second half of the table $\hat{o}_{1\uparrow} = c^\dagger_{1\uparrow}$ and $N' = N + 1$

$\hat{o}_{1\uparrow}\lvert N, S, S_z\rangle$			$w_1^\uparrow$	$E_n(N') - E_{n'}(N'-1)$
$c_{1\uparrow}\lvert 1, 1/2, \sigma\rangle_1$	$=$	$\delta_{\sigma,\uparrow}\lvert 0\rangle$	1	ε_d
$c_{1\uparrow}\lvert 2, 1, 0\rangle$	$=$	$\frac{1}{\sqrt{2}}c^\dagger_{2\downarrow}\lvert 0\rangle$	$\frac{1}{2}$	ε_d
$c_{1\uparrow}\lvert 2, 1, 1\rangle$	$=$	$-c^\dagger_{2\uparrow}\lvert 0\rangle$	1	ε_d
$c_{1\uparrow}\lvert 2, 0, 0\rangle_0$	$=$	$\frac{1}{\sqrt{2}}c^\dagger_{2\downarrow}\lvert 0\rangle$	$\frac{1}{2}$	ε_d
$c_{1\uparrow}\lvert 2, 0, 0\rangle_1$	$=$	$c^\dagger_{1\downarrow}\lvert 0\rangle$	1	$\varepsilon_d + U$
$c_{1\uparrow}\lvert 3, 1/2, \sigma\rangle_1$	$=$	$\delta_{\sigma,\uparrow}c^\dagger_{2\uparrow}c^\dagger_{2\downarrow}\lvert 0\rangle$	1	ε_d
$c_{1\uparrow}\lvert 3, 1/2, \sigma\rangle_2$	$=$	$-c^\dagger_{2\sigma}c^\dagger_{1\downarrow}\lvert 0\rangle$	1	$\varepsilon_d + U$
$c_{1\uparrow}\lvert 4, 0, 0\rangle$	$=$	$c^\dagger_{1\downarrow}c^\dagger_{2\uparrow}c^\dagger_{2\downarrow}\lvert 0\rangle$	1	$\varepsilon_d + U$
$c^\dagger_{1\uparrow}\lvert 0, 0, 0\rangle$	$=$	$c^\dagger_{1\uparrow}\lvert 0\rangle$	1	ε_d
$c^\dagger_{1\uparrow}\lvert 1, 1/2, \sigma\rangle_1$	$=$	$\delta_{\sigma,\downarrow}c^\dagger_{1\uparrow}c^\dagger_{1\sigma}\lvert 0\rangle$	1	$\varepsilon_d + U$
$c^\dagger_{1\uparrow}\lvert 1, 1/2, \sigma\rangle_2$	$=$	$c^\dagger_{1\uparrow}c^\dagger_{2\sigma}\lvert 0\rangle$	1	ε_d
$c^\dagger_{1\uparrow}\lvert 2, 1, 0\rangle$	$=$	$\frac{1}{\sqrt{2}}c^\dagger_{1\uparrow}c^\dagger_{1\downarrow}c^\dagger_{2\uparrow}\lvert 0\rangle$	$\frac{1}{2}$	$\varepsilon_d + U$
$c^\dagger_{1\uparrow}\lvert 2, 1, -1\rangle$	$=$	$-c^\dagger_{2\downarrow}c^\dagger_{1\uparrow}c^\dagger_{1\downarrow}\lvert 0\rangle$	1	$\varepsilon_d + U$
$c^\dagger_{1\uparrow}\lvert 2, 0, 0\rangle_0$	$=$	$-\frac{1}{\sqrt{2}}c^\dagger_{1\uparrow}c^\dagger_{1\downarrow}c^\dagger_{2\uparrow}\lvert 0\rangle$	$\frac{1}{2}$	$\varepsilon_d + U$
$c^\dagger_{1\uparrow}\lvert 2, 0, 0\rangle_2$	$=$	$c^\dagger_{1\uparrow}c^\dagger_{2\uparrow}c^\dagger_{2\downarrow}\lvert 0\rangle$	1	ε_d
$c^\dagger_{1\uparrow}\lvert 3, 1/2, \sigma\rangle_1$	$=$	$\delta_{\sigma,\downarrow}c^\dagger_{1\uparrow}c^\dagger_{1\sigma}c^\dagger_{2\uparrow}c^\dagger_{2\downarrow}\lvert 0\rangle$	1	$\varepsilon_d + U$

For $t \neq 0$ we have to recalculate the weights because the eigenstates are different. Let us first exploit the mirror symmetry of the Hamiltonian, however; thanks to it, any hermitian quadratic operator is diagonal in the basis of the bonding and anti-bonding state. Thus the local Green function can be expressed as the average of the bonding and antibonding one

$$G_{11,\sigma}(i\nu_n) = \frac{1}{2}\left[G_{++,\sigma} + G_{--,\sigma}\right]$$

where

$$G_{\pm\pm,\sigma}(i\nu_n) = -\int_0^\beta d\tau e^{i\nu_n\tau}\langle \mathcal{T} c_{\pm\sigma}(\tau)c^\dagger_{\pm\sigma}(0)\rangle,$$

and

$$c_{\pm\sigma} = \frac{1}{\sqrt{2}} \left(c_{1\uparrow} \mp c_{2\uparrow} \right).$$

For $U = 0$, the local Green function is thus simply

$$G^0_{11,\sigma}(i\nu_n) = \frac{1}{2} \sum_{\alpha=\pm} \frac{1}{i\nu_n - (\varepsilon_\alpha - \mu)} = \frac{1}{i\nu_n - (\varepsilon_d + F^0(i\nu_n) - \mu)},$$

where $\varepsilon_\pm = \varepsilon_d \pm t$. The quantity

$$F^0(i\nu_n) = \frac{t^2}{i\nu_n - (\varepsilon_d - \mu)},$$

is the so-called non-interacting hybridization function, and it can be seen as a self-energy for the uncorrelated atomic level ε_d. Let us now suppose that we are in the opposite limit, the one in which $4t \ll U$, and hence $E_-(2,0) \sim E_o(2,1)$. Furthermore, let us assume that $k_B T$ is much lower than the energy difference $E_o(2,0) - E_-(2,0)$; this implies that the two higher-energy states in the 2-electron sector can be neglected in calculating the Green function. In this limit the local Matsubara Green function is given by

$$G_{11,\sigma}(i\nu_n) \sim \frac{1}{4} \sum_{\alpha=\pm} \left[\frac{1}{i\nu_n - (\varepsilon_\alpha - \mu)} + \frac{1}{i\nu_n - (\varepsilon_\alpha + U - \mu)} \right]$$

$$= \frac{1}{2} \sum_{\alpha=\pm} \frac{1}{i\nu_n - (\varepsilon_\alpha - \mu + \Sigma_{\alpha\alpha}(i\nu_n))}.$$

The bonding and antibonding self-energy are

$$\Sigma_{\alpha\alpha}(i\nu_n) = \frac{U}{2} + \frac{U^2}{4} \frac{1}{i\nu_n - (\varepsilon_\alpha + \frac{1}{2}U - \mu)}.$$

In the large frequency limit, as will become clear later, the exact self-energy equals the Hartree-Fock self-energy for zero magnetization, $U/2$. The gap is given by

$$E^c_g = E_0(N+1) + E_0(N-1) - 2E_0(N) \sim U - 2t.$$

The formulas above show that the self-energy is different for the bonding and antibonding state. By making the analogy with an infinite tight-binding chain with dispersion $-2(t/2)\cos ka$, the bonding state corresponds to $k = 0$ and the anti-bonding state to $k = \pi/a$. Thus, in the lattice limit, our result reflects the fact that in general the self-energy depends on $\boldsymbol{k}$. In addition, the gap, which has the value U in the atomic limit, is reduced by the energy difference between antibonding and bonding state, $2t$; in the lattice limit, this difference becomes the band-width, W. The reason of the gap reduction is that, once we remove or add one electron, it does not cost Coulomb energy to move the hole/extra electron from one site to the other in the Hubbard dimer. Finally, we can rewrite the local Green function in a form that will become useful later

$$G_{11,\sigma}(i\nu_n) = \left[\frac{1}{i\nu_n - (\varepsilon_d - \mu + \Sigma_{l\sigma}(i\nu_n) + F_\sigma(i\nu_n))} \right]. \tag{6}$$

In this expression $\Sigma_l(i\nu_n)$ is the local self-energy

$$\begin{aligned}\Sigma_l(i\nu_n) =& \frac{1}{2}(\Sigma_{++}(i\nu_n) + \Sigma_{--}(i\nu_n)),\\ =& \frac{U}{2} + \frac{U^2}{4}\,\frac{1}{i\nu_n - (\varepsilon_d + \frac{1}{2}U - \mu + \frac{t^2}{(i\nu_n - (\varepsilon_d + \frac{1}{2}U - \mu))})},\end{aligned}$$

and $F_\sigma(i\nu_n)$ the hybridization function for the correlated dimer

$$F_\sigma(i\nu_n) = \frac{(t + \Delta\Sigma_l(i\nu_n))^2}{i\nu_n - (\varepsilon_d - \mu + \Sigma_{l\sigma}(i\nu_n))}.$$

The difference

$$\begin{aligned}\Delta\Sigma_{l\sigma}(i\nu_n) =& \frac{1}{2}(\Sigma_{++}(i\nu_n) - \Sigma_{--}(i\nu_n))\\ =& \frac{U^2}{4}\,\frac{t}{(i\nu_n - (\varepsilon_d + \frac{1}{2}U - \mu))^2 - t^2},\end{aligned}$$

measures the strength of non-local effects. The sum $F_l(i\nu_n) + \Sigma_l(i\nu_n)$ yields the total modification of the isolated ($t = 0$) and uncorrelated ($U = 0$) level ε_d. Later we will compare expression (6) to its analogous for another simple model, the Anderson molecule.

2.2.3 Long-range Coulomb interaction

A natural question that follows is: what happens if the Coulomb repulsion is longer range? For a dimer, extending the Coulomb interaction to first neighbors leads to the Hamiltonian

$$\begin{aligned}\hat{H} =& \varepsilon_d \sum_{i\sigma} \hat{n}_{i\sigma} - t \sum_{\sigma} \left[c^\dagger_{1\sigma} c_{2\sigma} + c^\dagger_{2\sigma} c_{1\sigma}\right] + U \sum_{i=1,2} \hat{n}_{i\uparrow}\hat{n}_{i\downarrow}\\ &+ \sum_{\sigma\neq\sigma'} (V - 2J_V - J_V\delta_{\sigma\sigma'})\hat{n}_{1\sigma}\hat{n}_{2\sigma'} - J_V \sum_{i\neq i'} \left[c^\dagger_{i\uparrow} c_{i\downarrow} c^\dagger_{i'\downarrow} c_{i'\uparrow} + c^\dagger_{i'\uparrow} c^\dagger_{i'\downarrow} c_{i\uparrow} c_{i\downarrow}\right],\end{aligned}$$

where the parameters in the last two terms are the intersite direct (V) and exchange (J_V) Coulomb interaction. For two electrons the Hamiltonian becomes

$$\hat{H}_2 = \begin{pmatrix} 2\varepsilon_d + V - 3J_V & 0 & 0 & 0 & 0 & 0\\ 0 & 2\varepsilon_d + V - 3J_V & 0 & 0 & 0 & 0\\ 0 & 0 & 2\varepsilon_d + V - 3J_V & 0 & 0 & 0\\ 0 & 0 & 0 & 2\varepsilon_d + V - J_V & -\sqrt{2}t & -\sqrt{2}t\\ 0 & 0 & 0 & -\sqrt{2}t & 2\varepsilon_d + U & -J_V\\ 0 & 0 & 0 & -\sqrt{2}t & -J_V & 2\varepsilon_d + U \end{pmatrix}.$$

Thus, if $J_V = 0$, apart from an irrelevant shift, the Hamiltonian at half-filling equals the $\hat{H}_2$ matrix that we obtained for $V = 0$, provided that in the latter U is replaced by $U - V$; hence the

V term effectively reduces the strength of the local Coulomb interaction and at the same time enhances the exchange coupling, which becomes $\Gamma \sim 4t^2/(U-V)$. What about the charge gap? Let us calculate the gap exactly, without assuming $4t \ll U$ as we have done previously. This leads to the formula

$$E_g^c(V) = -2t + V + \sqrt{(U-V)^2 + 16t^2}.$$

Let us consider the case in which $4t/U$ is small. There are two interesting limits. The first, $V/U \to 0$, yield the previous result, $E_g(V) \sim U - 2t$. The second is $V/U \sim 1$, which gives $E_g(V) \sim 2t+V$. In this case the gap equals the one of an uncorrelated dimer with enhanced hopping integrals, $t \to t+V/2$. In this limit, the elements of the matrices $\hat{H}_N$ are basically identical to those we obtained for $U = V = J_V = 0$, apart for a shift on the diagonal; thus also the eigenstates are close to those of the non-interacting dimer. Although for realistic lattices the effect of V is more complex [11], the simple result above explains why actual strong-correlation effects mostly appear when the local Coulomb coupling is large compared to longer-range terms.

2.2.4 Hartree-Fock approximation

Let us now compare the exact solution of the Hubbard dimer with the result of the Hartree-Fock approximation. Here we return for simplicity to the case $V = J_V = 0$. The Hartree-Fock Hamiltonian can be obtained by replacing

$$\hat{H}_U = U \sum_i \hat{n}_{i\uparrow}\hat{n}_{i\downarrow} \to \hat{H}_U^{\rm HF} = U \sum_i [\hat{n}_{i\uparrow}\bar{n}_{i\downarrow} + \hat{n}_{i\downarrow}\bar{n}_{i\uparrow} - \bar{n}_{i\uparrow}\bar{n}_{i\downarrow}], \tag{7}$$

where $\bar{n}_{i\sigma}$ is the HF expectation value of the operator $\hat{n}_{i\sigma}$. Thus we have

$$\hat{H}^{\rm HF} = \varepsilon_d \sum_{i\sigma} \hat{n}_{i\sigma} - t \sum_\sigma \left[c_{1\sigma}^\dagger c_{2\sigma} + c_{2\sigma}^\dagger c_{1\sigma}\right] + U \sum_{\sigma\neq\sigma'} [\hat{n}_{1\sigma}\bar{n}_{1\sigma'} + \hat{n}_{2\sigma}\bar{n}_{2\sigma'}] - U \sum_i \bar{n}_{i\uparrow}\bar{n}_{i\downarrow}.$$

It is convenient to introduce the quantities

$$n_i = \bar{n}_{i\uparrow} + \bar{n}_{i\downarrow} \qquad n = \frac{1}{2}(n_1 + n_2) \qquad \delta n = \frac{1}{2}(n_1 - n_2)$$
$$m_i = \frac{1}{2}(\bar{n}_{i\uparrow} - \bar{n}_{i\downarrow}) \qquad m_+ = \frac{1}{2}(m_1 + m_2) \qquad m_- = \frac{1}{2}(m_1 - m_2)$$

Inverting these relations

$$n_{1\uparrow} = (m_+ + m_-) + (n + \delta n)/2 \qquad n_{1\downarrow} = -(m_+ + m_-) + (n + \delta n)/2$$
$$n_{2\uparrow} = (m_+ - m_-) + (n - \delta n)/2 \qquad n_{2\downarrow} = -(m_+ - m_-) + (n - \delta n)/2$$

The Hartree-Fock version of the Hubbard dimer Hamiltonian equals the non-interacting Hamiltonian plus a shift of the on-site level. This shift depends on the site and the spin

$$\begin{aligned}\hat{H}_{\mathrm{HF}} &= \sum_{i\sigma} \left(\varepsilon_d + \Delta_{i\sigma}\right) \hat{n}_{i\sigma} - t \sum_{\sigma} \left(c^{\dagger}_{1\sigma} c_{2\sigma} + c^{\dagger}_{2\sigma} c_{1\sigma} \right) - \Delta_0 \\ \Delta_0 &= 2U \left[\frac{n^2 + \delta n^2}{4} - m_+^2 - m_-^2 \right] \\ \Delta_{i\sigma} &= U \left[(-1)^{\sigma} \left(m_+ + (-1)^{i-1} m_- \right) + \frac{1}{2} (n + (-1)^{i-1} \delta n) \right].\end{aligned}$$

Thus we can write immediately the local Green function matrix for site 1. It is convenient to use this time the site basis, hence, to calculate the matrix $G_{ii',\sigma}(i\nu_n)$. Then we have

$$G_{11,\sigma}(i\nu_n) = \left[\begin{array}{cc} i\nu_n - (\varepsilon_d - \mu + \Sigma_{11,\sigma}(i\nu_n)) & t \\ t & i\nu_n - (\varepsilon_d - \mu + \Sigma_{22,\sigma}(i\nu_n)) \end{array} \right]^{-1}_{11}$$

where

$$\Sigma_{ii,\sigma}(i\nu_n) = \Delta_{i\sigma}.$$

This shows that the self-energy is not dependent on the frequency, i.e., Hartree-Fock is a *static* mean-field approach. The value of the parameters m_+, m_- and δn have to be found solving the system of self-consistent equations given by

$$\bar{n}_{i\sigma} = \frac{1}{\beta} \sum_n e^{-i\nu_n 0^-} G_{ii,\sigma}(i\nu_n).$$

For ferromagnetic (F) and antiferromagnetic (AF) solutions we have, in the absence of charge disproportionation, the following simplifications

$$\begin{aligned}\Delta^{\mathrm{F}}_{1\sigma} &= U \left(\frac{n}{2} + \sigma m_+ \right) & \Delta^{\mathrm{AF}}_{1\sigma} &= U \left(\frac{n}{2} + \sigma m_- \right) \\ \Delta^{\mathrm{F}}_{2\sigma} &= U \left(\frac{n}{2} + \sigma m_+ \right) & \Delta^{\mathrm{AF}}_{2\sigma} &= U \left(\frac{n}{2} - \sigma m_- \right)\end{aligned}$$

In the AF case, the self-energy depends on the site. In the lattice limit, this implies that the interaction couples $\boldsymbol{k}$ states. Indeed, by rewriting the Green-function matrix in the basis of the bonding ($k = 0$) and anti-bonding ($k = \pi$) creation/annihilation operators we have

$$G_{\sigma}(i\nu_n) = \frac{1}{2} \left[\begin{array}{cc} i\nu_n - (\varepsilon_d - t - \mu + \frac{1}{2}\sum_i \Sigma_{i\sigma}(i\nu_n)) & \frac{1}{2}\sum_i (-1)^{i-1} \Sigma_{i\sigma}(i\nu_n) \\ \frac{1}{2}\sum_i (-1)^{i-1} \Sigma_{i\sigma}(i\nu_n) & i\nu_n - (\varepsilon_d + t - \mu + \frac{1}{2}\sum_i \Sigma_{i\sigma}(i\nu_n)) \end{array} \right]^{-1}.$$

The diagonal terms are identical, hence

$$\Sigma_{++,\sigma}(i\nu_n) = \Sigma_{--,\sigma}(i\nu_n) = \Sigma_l(i\nu_n).$$

The off-diagonal terms $\Sigma_{+-}(i\nu_n)$ and $G_{+-}(i\nu_n)$ are not zero, however. This tells us that, by introducing the HF correction, we can lower the symmetry of the system. Let us now calculate

explicitly the eigenstates for different fillings. For this it is sufficient to diagonalize $\hat{H}_1$, the Hamiltonian in the 1-electron sector; the many-electron states can be obtained by filling the one-electron states via the Pauli principle. The Hamiltonian $\hat{H}_1$ can be written as $\hat{H}_1 = \hat{H}_1' + \varepsilon_d \hat{N} - \Delta_0$, and, in the AF case we then have

$$\hat{H}_1' = \begin{pmatrix} U(\frac{1}{2}n - m_-) & -t & 0 & 0 \\ -t & U(\frac{1}{2}n + m_-) & 0 & 0 \\ 0 & 0 & U(\frac{1}{2}n + m_-) & -t \\ 0 & 0 & -t & U(\frac{1}{2}n - m_-) \end{pmatrix}.$$

This leads to the (normalized) states

$\|1\rangle_l$	$E_l(1)$
$\|1\rangle_3 = a_2\|1,1/2,\uparrow\rangle_1 - a_1\|1,1/2,\uparrow\rangle_2$	$\varepsilon_0(1) + \Delta_1(t,U)$
$\|1\rangle_2 = a_1\|1,1/2,\downarrow\rangle_1 - a_2\|1,1/2,\downarrow\rangle_2$	$\varepsilon_0(1) + \Delta_1(t,U)$
$\|1\rangle_1 = a_1\|1,1/2,\uparrow\rangle_1 + a_2\|1,1/2,\uparrow\rangle_2$	$\varepsilon_0(1) - \Delta_1(t,U)$
$\|1\rangle_0 = a_2\|1,1/2,\downarrow\rangle_1 + a_1\|1,1/2,\downarrow\rangle_2$	$\varepsilon_0(1) - \Delta_1(t,U)$

where $\varepsilon_0(1) = \varepsilon_d + U(1/2 + 2m_-^2 - n^2/2)$ and $a_1^2 = \frac{1}{2}\left(1 + \frac{Um_-}{\Delta_1(t,U)}\right)$. The charge gap at half filling is

$$E_g^{\rm HF} = 2\Delta_1(t,U) = 2\sqrt{(m_- U)^2 + t^2}.$$

In general the Hartree-Fock gap tends to be larger than the exact value. If we assume that only the ground state is occupied, solving the self-consistent equations yields the solutions

$$m_- = 0 \quad \text{or} \quad m_- = \frac{1}{2}\sqrt{1 - \frac{4t^2}{U^2}}.$$

Using this result we find $E_g^{\rm HF} = U$. It is useful to look more in detail at $\hat{H}_2'$, with $\hat{H}_2 = \hat{H}_2' + \varepsilon_d \hat{N} - \Delta_0$; in the absence of charge disproportionation, it has the general form

$$\hat{H}_2' = \begin{pmatrix} U & 0 & 0 & -2Um_- & 0 & 0 \\ 0 & U(1-2m_+) & 0 & 0 & 0 & 0 \\ 0 & 0 & U(1+2m_+) & 0 & 0 & 0 \\ -2Um_- & 0 & 0 & U & -\sqrt{2}t & -\sqrt{2}t \\ 0 & 0 & 0 & -\sqrt{2}t & U & 0 \\ 0 & 0 & 0 & -\sqrt{2}t & 0 & U \end{pmatrix}$$

If we search for an AF solution, the normalized Hartree-Fock eigenvalues and eigenvectors are

$\|2\rangle_l$	$E_l(2)$
$\|2\rangle_5 = \frac{1}{\sqrt{2}}\left[\|2,0,0\rangle_0 + a_2\|2,1,0\rangle - \frac{a_1}{\sqrt{2}}\left[\|2,0,0\rangle_1 + \|2,0,0\rangle_2\right]\right]$	$\varepsilon_0(2) + 2\Delta_1(t,U)$
$\|2\rangle_4 = \frac{1}{\sqrt{2}}\left[\|2,0,0\rangle_1 - \|2,0,0\rangle_2\right]$	$\varepsilon_0(2)$
$\|2\rangle_3 = \|2,1,1\rangle$	$\varepsilon_0(2)$
$\|2\rangle_2 = \|2,1,-1\rangle$	$\varepsilon_0(2)$
$\|2\rangle_1 = a_1\|2,1,0\rangle + a_2\frac{1}{\sqrt{2}}\left[\|2,0,0\rangle_1 + \|2,0,0\rangle_2\right]$	$\varepsilon_0(2)$
$\|2\rangle_0 = \frac{1}{\sqrt{2}}\left[\|2,0,0\rangle_0 - a_2\|2,1,0\rangle + \frac{a_1}{\sqrt{2}}\left[\|2,0,0\rangle_1 + \|2,0,0\rangle_2\right]\right]$	$\varepsilon_0(2) - 2\Delta_1(t,U)$

where $\varepsilon_0(2) = 2\varepsilon_d + U(1 + 2m_-^2 - n^2/2)$, and $a_1^2 = t^2/\Delta_1^2(t,U)$. There are several observations to make. The Hartree-Fock ground state has an overlap with the correct ground state, however incorrectly mixes triplet and singlet states, thus breaking the rotational symmetry of the model. For this reason, its energy, in the large U limit, is $2\varepsilon_d - 2t^2/U$ and not $2\varepsilon_d - 4t^2/U$ as in the exact case. For a F solution, the eigenvalues and eigenvectors are

$\|2\rangle_l$	$E_l(2)$
$\|2\rangle_5 = \|2,1,-1\rangle$	$\varepsilon_0^+(2) + 2Um_+$
$\|2\rangle_4 = \frac{1}{\sqrt{2}}\left[\|2,0,0\rangle_0 - \frac{1}{\sqrt{2}}\left[\|2,0,0\rangle_1 + \|2,0,0\rangle_2\right]\right]$	$\varepsilon_0^+(2) + 2t$
$\|2\rangle_3 = \frac{1}{\sqrt{2}}\left[\|2,0,0\rangle_1 - \|2,0,0\rangle_2\right]$	$\varepsilon_0^+(2)$
$\|2\rangle_2 = \|2,1,\quad 0\rangle$	$\varepsilon_0^+(2)$
$\|2\rangle_1 = \frac{1}{\sqrt{2}}\left[\|2,0,0\rangle_0 + \frac{1}{\sqrt{2}}\left[\|2,0,0\rangle_1 + \|2,0,0\rangle_2\right]\right]$	$\varepsilon_0^+(2) - 2t$
$\|2\rangle_0 = \|2,1,\quad 1\rangle$	$\varepsilon_0^+(2) - 2Um_+$

where $\varepsilon_0^+(2) = 2\varepsilon_d + U(1 + 2m_+^2 - n^2/2)$. The ferromagnetic Hartree-Fock correction thus yields an incorrect sequence of levels; the ground state for large U/t, indicated as $|2\rangle_0$ in the table, has no overlap with the exact ground state of the Hubbard dimer. It is, instead, one of the states of the first excited triplet. The energy difference between F- and AF-magnetic ground state is

$$E_{AF} - E_F \sim -\frac{2t^2}{U},$$

which is indeed the exact energy difference between antiferromagnetic and ferromagnetic state. It does not correspond, however, to the actual singlet-triplet excitation energy, $\Gamma \sim 4t^2/U$.

3 The Anderson model

3.1 Introduction

A magnetic impurity in a metallic host can be described by the Anderson model

$$\hat{H}_{\rm A} = \underbrace{\sum_{\sigma}\sum_{\boldsymbol{k}} \varepsilon_{\boldsymbol{k}} n_{\boldsymbol{k}\sigma} + \sum_{\sigma} \varepsilon_f\, \hat{n}_{f\sigma} + U \hat{n}_{f\uparrow}\hat{n}_{f\downarrow}}_{\hat{H}_0} + \underbrace{\sum_{\sigma}\sum_{\boldsymbol{k}} \left[V_{\boldsymbol{k}} c^{\dagger}_{\boldsymbol{k}\sigma} c_{f\sigma} + h.c. \right]}_{\hat{H}_1},$$

where ε_f is the impurity level (occupied by $n_f \sim 1$ electrons), $\varepsilon_{\boldsymbol{k}}$ is the dispersion of the metallic band, and $V_{\boldsymbol{k}}$ the hybridization. If we assume that the system has particle-hole symmetry with respect to the Fermi level, then $\varepsilon_f - \mu = -U/2$. The Kondo regime is characterized by the parameter values $\varepsilon_f \ll \mu$ and $\varepsilon_f + U \gg \mu$ and by a weak hybridization, i.e., the hybridization width, which is the imaginary part of the hybridization function for the Anderson model,

$$\Delta(\varepsilon) = \pi \frac{1}{N_{\boldsymbol{k}}} \sum_{\boldsymbol{k}} |V_{\boldsymbol{k}}|^2 \delta(\varepsilon_{\boldsymbol{k}} - \varepsilon)$$

is such that $\Delta(\mu) \ll |\mu - \varepsilon_f|, |\mu - \varepsilon_f - U|$. The Anderson model is important in this lecture because it is used as quantum-impurity model in dynamical mean-field theory. Through the Schrieffer-Wolff canonical transformation [10] one can map the Anderson model onto the Kondo model, in which only the effective spin of the impurity enters

$$\hat{H}_{\rm K} = \hat{H}'_0 + \Gamma \boldsymbol{S}_f \cdot \boldsymbol{s}_c(\boldsymbol{0}) = \hat{H}'_0 + \hat{H}_{\Gamma}, \tag{8}$$

where

$$\Gamma \sim -2|V_{k_F}|^2 \left[\frac{1}{\varepsilon_f} - \frac{1}{\varepsilon_f + U} \right] > 0$$

is the antiferromagnetic coupling arising from the hybridization, $\boldsymbol{S}_f$ the spin of the impurity ($S_f = 1/2$), and $\boldsymbol{s}_c(\boldsymbol{0})$ is the spin-density of the conduction band at the impurity site. For convenience we set the Fermi energy to zero; k_F is a $\boldsymbol{k}$ vector at the Fermi level. The Schrieffer-Wolff canonical transformation works as follows. We introduce the operator $\hat{S}$ that transforms the Hamiltonian $\hat{H}$ into $\hat{H}_S$

$$\hat{H}_S = e^{\hat{S}} \hat{H} e^{-\hat{S}}.$$

We search for an operator $\hat{S}$ such that the transformed Hamiltonian $\hat{H}_S$ has no terms of first order in $V_{\boldsymbol{k}}$. Let us first split the original Hamiltonian $\hat{H}_A$ into two pieces: $\hat{H}_0$, the sum of all terms except the hybridization term, and $\hat{H}_1$, the hybridization term. Let us choose $\hat{S}$ linear in $V_{\boldsymbol{k}}$ and such that

$$[\hat{S}, \hat{H}_0] = -\hat{H}_1. \tag{9}$$

From Eq. (9) one finds that the operator $\hat{S}$ is given by

$$\hat{S} = \sum_{\boldsymbol{k}\sigma} \left[\frac{1-\hat{n}_{f-\sigma}}{\varepsilon_{\boldsymbol{k}} - \varepsilon_f} + \frac{\hat{n}_{f-\sigma}}{\varepsilon_{\boldsymbol{k}} - \varepsilon_f - U} \right] V_{\boldsymbol{k}} c^\dagger_{\boldsymbol{k}\sigma} c_{f\sigma} - \text{h.c.}.$$

The transformed Hamiltonian is complicated, as can be seen from explicitly writing the series for a transformation satisfying Eq. (9)

$$\hat{H}_S = \hat{H}_0 + \frac{1}{2}\left[\hat{S}, \hat{H}_1\right] + \frac{1}{3}\Big[\hat{S}, \left[\hat{S}, \hat{H}_1\right]\Big] + \dots.$$

In the limit in which the hybridization strength Γ is small this series can, however, be truncated at second order. The resulting Hamiltonian has the form

$$\hat{H}_S = \hat{H}_0 + \hat{H}_2,$$

with

$$\hat{H}_2 = \hat{H}_\Gamma + \hat{H}_{\text{dir}} + \Delta\hat{H}_0 + \hat{H}_{\text{ch}}.$$

The first term is the exchange interaction

$$\hat{H}_\Gamma = \frac{1}{4}\sum_{\boldsymbol{k}\boldsymbol{k}'} \Gamma_{\boldsymbol{k}\boldsymbol{k}'} \left[\sum_{\sigma_1\sigma_2} c^\dagger_{\boldsymbol{k}'\sigma_1} \langle\sigma_1|\hat{\sigma}|\sigma_2\rangle c_{\boldsymbol{k}\sigma_2} \cdot \sum_{\sigma_3\sigma_4} c^\dagger_{f\sigma_3} \langle\sigma_3|\hat{\sigma}|\sigma_4\rangle c_{f\sigma_4} \right]$$

where

$$\Gamma_{\boldsymbol{k}\boldsymbol{k}'} = V^*_{\boldsymbol{k}} V_{\boldsymbol{k}'} \left[\frac{1}{\varepsilon_{\boldsymbol{k}} - \varepsilon_f} + \frac{1}{\varepsilon_{\boldsymbol{k}'} - \varepsilon_f} + \frac{1}{U + \varepsilon_f - \varepsilon_{\boldsymbol{k}}} + \frac{1}{U + \varepsilon_f - \varepsilon_{\boldsymbol{k}'}} \right].$$

Let us assume that the coupling $\Gamma_{\boldsymbol{k}\boldsymbol{k}'}$ is weakly dependent on $\boldsymbol{k}$ and $\boldsymbol{k}'$; then by setting $|\boldsymbol{k}| \sim k_F$, and $|\boldsymbol{k}'| \sim k_F$ we recover the antiferromagnetic contact coupling in Eq. (8).
The second term is a potential-scattering interaction

$$\hat{H}_{\text{dir}} = \sum_{\boldsymbol{k}\boldsymbol{k}'} \left[A_{\boldsymbol{k}\boldsymbol{k}'} - \frac{1}{4}\Gamma_{\boldsymbol{k}\boldsymbol{k}'}\hat{n}_f \right] \sum_\sigma \hat{c}^\dagger_{\boldsymbol{k}'\sigma}\hat{c}_{\boldsymbol{k}\sigma},$$

where

$$A_{\boldsymbol{k}\boldsymbol{k}'} = \frac{1}{2} V^*_{\boldsymbol{k}} V_{\boldsymbol{k}'} \left[\frac{1}{\varepsilon_{\boldsymbol{k}} - \varepsilon_f} + \frac{1}{\varepsilon_{\boldsymbol{k}'} - \varepsilon_f} \right].$$

This term is spin-independent, and thus does not play a relevant role in the Kondo effect. The next term merely modifies the $\hat{H}_0$ term

$$\Delta\hat{H}_0 = -\sum_{\boldsymbol{k}\sigma} \left[A_{\boldsymbol{k}\boldsymbol{k}} - \frac{1}{2}\Gamma_{\boldsymbol{k}\boldsymbol{k}}\, \hat{n}_{f-\sigma} \right] \hat{n}_{f\sigma}.$$

Finally, the last term is a pair-hopping interaction, which changes the charge of the f site by two electrons and thus can be neglected if $n_f \sim 1$

$$\Delta\hat{H}_{\text{ch}} = -\frac{1}{4}\sum_{\boldsymbol{k}\boldsymbol{k}'\sigma} \Gamma_{\boldsymbol{k}\boldsymbol{k}'} c^\dagger_{\boldsymbol{k}'-\sigma} c^\dagger_{\boldsymbol{k}\sigma} c_{f\sigma} c_{f-\sigma} + \text{h.c.}.$$

The essential term in $\hat{H}_2$ is the exchange term $\hat{H}_\Gamma$, which is the one that yields the antiferromagnetic contact interaction in the Kondo Hamiltonian (8).

3.1.1 Poor man's scaling

We can understand the nature of the ground state of the Kondo model by using a simple approach due to Anderson called *poor man's scaling* [13] and an argument due to Nozières. First we divide the Hilbert space into a high- and a low-energy sector. We define as *high-energy* states those with at least one electron or one hole at the top or bottom of the band; the corresponding constraint for the high-energy electronic level $\varepsilon_{\boldsymbol{q}}$ is $D' < \varepsilon_{\boldsymbol{q}} < D$ or $-D < \varepsilon_{\boldsymbol{q}} < -D'$, where $D' = D - \delta D$. Next we introduce the operator $\hat{P}_H$, which projects onto the high-energy states, and the operator $\hat{P}_L = \hat{1} - \hat{P}_H$, which projects onto states with no electrons or holes in the high-energy region. Then we downfold the high-energy sector of the Hilbert space. To do this we rewrite the original Kondo Hamiltonian,

$$\hat{H} \equiv \hat{H}'_0 + \hat{H}_\Gamma,$$

as the energy-dependent operator $\hat{H}'$, which acts only in the low-energy sector

$$\hat{H}' = \hat{P}_L \hat{H} \hat{P}_L + \delta\hat{H}_L = \hat{H}_L + \delta\hat{H}_L,$$
$$\delta\hat{H}_L = \hat{P}_L \hat{H} \hat{P}_H \left(\omega - \hat{P}_H \hat{H} \hat{P}_H\right)^{-1} \hat{P}_H \hat{H} \hat{P}_L.$$

Here $\hat{H}_L$ is the original Hamiltonian, however in the space in which the high-energy states have been downfolded; the term $\delta\hat{H}_L$ is a correction due to the interaction between low-energy and (downfolded) high-energy states. Up to this point, the operator $\hat{H}'$ has the same spectrum as the original Hamiltonian. To make use of this expression, however, we have to introduce approximations. Thus, let us calculate $\delta\hat{H}_L$ using many-body perturbation theory. The first non-zero contribution is of second order in Γ

$$\delta\hat{H}_L^{(2)} \sim \hat{P}_L \hat{H}_\Gamma \hat{P}_H \left(\omega - \hat{P}_H \hat{H}'_0 \hat{P}_H\right)^{-1} \hat{P}_H \hat{H}_\Gamma P_L \,.$$

There are two types of processes that contribute at the second order, an electron and a hole process, depending on whether the downfolded states have (at least) one electron or one hole in the high-energy region. Let us consider the electron process. We set

$$\hat{P}_H \sim \sum_{\boldsymbol{q}\sigma} c^\dagger_{\boldsymbol{q}\sigma} |FS\rangle\langle FS| c_{\boldsymbol{q}\sigma},$$

$$\hat{P}_L \sim \sum_{\boldsymbol{k}\sigma} c^\dagger_{\boldsymbol{k}\sigma} |FS\rangle\langle FS| c_{\boldsymbol{k}\sigma} \,,$$

where $|\varepsilon_{\boldsymbol{k}}| < D'$ and

$$|FS\rangle = \prod_{\boldsymbol{k}\sigma} c^\dagger_{\boldsymbol{k}\sigma} |0\rangle$$

is the Fermi sea, i.e., the many-body state corresponding to the metallic conduction band. Thus

$$\delta H_L^{(2)} = -\frac{1}{2}\Gamma^2 \sum_{\boldsymbol{q}} \frac{1}{\omega - \varepsilon_{\boldsymbol{q}}} \boldsymbol{S}_f \cdot \boldsymbol{s}_c(\boldsymbol{0}) + \ldots$$

$$\sim \frac{1}{4}\rho(\varepsilon_F)\Gamma^2 \frac{\delta D}{D} \boldsymbol{S}_f \cdot \boldsymbol{s}_c(\boldsymbol{0}) + \ldots .$$

We find an analogous contribution from the hole process. The correction $\delta H_L^{(2)}$ modifies the parameter Γ of the Kondo Hamiltonian as follows

$$\Gamma \to \Gamma' = \Gamma + \delta\Gamma,$$

and

$$\frac{\delta\Gamma}{\delta \ln D} = \frac{1}{2}\rho(\varepsilon_F)\Gamma^2, \tag{10}$$

where

$$\delta \ln D = \delta D/D.$$

It can be seen that equation (10) has two fixed points

(i) $\Gamma = 0$ (*weak coupling*)

(ii) $\Gamma \to \infty$ (*strong coupling*)

By solving the scaling equation we find

$$\Gamma' = \frac{\Gamma}{1 + \frac{1}{2}\rho(\varepsilon_F)\Gamma \ln \frac{D'}{D}} \ .$$

If the original coupling Γ is antiferromagnetic, the renormalized coupling constant Γ' diverges (i.e., it scales to the strong coupling fixed point) for

$$D' = De^{-2/\Gamma\rho(\varepsilon_F)}.$$

We can define this value of D' as the Kondo energy

$$k_B T_{\mathrm{K}} = De^{-2/\Gamma\rho(\varepsilon_F)}. \tag{11}$$

The divergence at $k_B T_{\mathrm{K}}$ indicates that at low energy the interaction between the spins dominates, and therefore the system forms a singlet in which the impurity magnetic moment is screened. The existence of this strong coupling fixed point is confirmed by the numerical renormalization group of Wilson [14]. Nozières [15] has used this conclusion to show that the low-temperature behavior of the system must be of Fermi liquid type. His argument is the following. For infinite coupling Γ' the impurity traps a conduction electron to form a singlet state. For a finite but still very large Γ', any attempt at breaking the singlet will cost a very large energy. Virtual excitations (into the $n_f = 0$ or $n_f = 2$ states and finally the $n_f = 1$ triplet state) are, however, possible and they yield an effective indirect interaction between the remaining conduction electrons surrounding the impurity. This is similar to the phonon-mediated attractive interaction in metals. The indirect electron-electron coupling is weak and can be calculated in perturbation theory ($1/\Gamma$ expansion). Nozières has shown that, to first approximation, the effective interaction is between electrons of opposite spins lying next to the impurity. It is of order D^4/Γ^3 and repulsive, hence it gives rise to a Fermi liquid behavior with enhanced susceptibility [15].

3.2 The Anderson molecule

As in the case of the Hubbard model, it is useful to look at a simpler case, the Anderson molecule. The corresponding Hamiltonian is given by

$$\hat{H} = \varepsilon_f \, \hat{n}_{1\sigma} + \varepsilon_s \hat{n}_{2\sigma} - t_A \sum_\sigma \left[c^\dagger_{1\sigma} c_{2\sigma} + c^\dagger_{2\sigma} c_{1\sigma} \right] + U \hat{n}_{1\uparrow} \hat{n}_{1\downarrow}. \tag{12}$$

Also this Hamiltonian commutes with the number of electron operator $\hat{N}$, with the total spin $\hat{S}$ and with $\hat{S}_z$. Thus we can express the states in the atomic limit as

$\lvert N, S, S_z \rangle$			N	S	$E(N)$
$\lvert 0,0,0 \rangle$	$=$	$\lvert 0 \rangle$	0	0	0
$\lvert 1,1/2,\sigma \rangle_1$	$=$	$c^\dagger_{1\sigma} \lvert 0 \rangle$	1	$1/2$	ε_f
$\lvert 1,1/2,\sigma \rangle_2$	$=$	$c^\dagger_{2\sigma} \lvert 0 \rangle$	1	$1/2$	ε_s
$\lvert 2,1,0 \rangle$	$=$	$\frac{1}{\sqrt{2}} \left[c^\dagger_{1\uparrow} c^\dagger_{2\downarrow} + c^\dagger_{1\downarrow} c^\dagger_{2\uparrow} \right] \lvert 0 \rangle$	2	1	$\varepsilon_f + \varepsilon_s$
$\lvert 2,1,1 \rangle$	$=$	$c^\dagger_{2\uparrow} c^\dagger_{1\uparrow} \lvert 0 \rangle$	2	1	$\varepsilon_f + \varepsilon_s$
$\lvert 2,1,-1 \rangle$	$=$	$c^\dagger_{2\downarrow} c^\dagger_{1\downarrow} \lvert 0 \rangle$	2	1	$\varepsilon_f + \varepsilon_s$
$\lvert 2,0,0 \rangle_0$	$=$	$\frac{1}{\sqrt{2}} \left[c^\dagger_{1\uparrow} c^\dagger_{2\downarrow} - c^\dagger_{1\downarrow} c^\dagger_{2\uparrow} \right] \lvert 0 \rangle$	2	0	$\varepsilon_f + \varepsilon_s$
$\lvert 2,0,0 \rangle_1$	$=$	$c^\dagger_{1\uparrow} c^\dagger_{1\downarrow} \lvert 0 \rangle$	2	0	$2\varepsilon_f + U$
$\lvert 2,0,0 \rangle_2$	$=$	$c^\dagger_{2\uparrow} c^\dagger_{2\downarrow} \lvert 0 \rangle$	2	0	$2\varepsilon_s$
$\lvert 3,1/2,\sigma \rangle_1$	$=$	$c^\dagger_{1\sigma} c^\dagger_{2\uparrow} c^\dagger_{2\downarrow} \lvert 0 \rangle$	3	$1/2$	$\varepsilon_f + 2\varepsilon_s$
$\lvert 3,1/2,\sigma \rangle_2$	$=$	$c^\dagger_{2\sigma} c^\dagger_{1\uparrow} c^\dagger_{1\downarrow} \lvert 0 \rangle$	3	$1/2$	$2\varepsilon_f + \varepsilon_s + U$
$\lvert 4,0,0 \rangle$	$=$	$c^\dagger_{1\uparrow} c^\dagger_{1\downarrow} c^\dagger_{2\uparrow} c^\dagger_{2\downarrow} \lvert 0 \rangle$	4	0	$2\varepsilon_f + 2\varepsilon_s + U$

Again, for $N = 2$ electrons, the hopping integrals only couple the $S = 0$ states. The Hamiltonian looks like

$$\hat{H}_2 = \begin{pmatrix} \varepsilon_f + \varepsilon_s & 0 & 0 & 0 & 0 & 0 \\ 0 & \varepsilon_f + \varepsilon_s & 0 & 0 & 0 & 0 \\ 0 & 0 & \varepsilon_f + \varepsilon_s & 0 & 0 & 0 \\ 0 & 0 & 0 & \varepsilon_f + \varepsilon_s & -\sqrt{2} t_A & -\sqrt{2} t_A \\ 0 & 0 & 0 & -\sqrt{2} t_A & 2\varepsilon_f + U & 0 \\ 0 & 0 & 0 & -\sqrt{2} t_A & 0 & 2\varepsilon_s \end{pmatrix}$$

The ground-state is a singlet, as in the Kondo problem. In order to calculate its energy, let us downfold the doubly-occupied states. We find

$$E_0(\omega) = \omega = \varepsilon_f + \varepsilon_s - \frac{2t_A^2}{2\varepsilon_f + U - \omega} - \frac{2t_A^2}{2\varepsilon_s - \omega}.$$

If we set $\omega = \varepsilon_f + \varepsilon_s - \Delta E$, and $\varepsilon_s \sim 0$ we have the solution

$$\Delta E \sim -2t_A^2 \left[\frac{1}{\varepsilon_f} - \frac{1}{\varepsilon_f + U}\right] \equiv \Gamma.$$

We can define ΔE as Kondo energy for the Anderson molecule. There is an important difference with respect to the real Kondo model, namely that in that case the Kondo energy, defined in Eq. (11), decreases exponentially with the inverse of Γ. The non-perturbative nature of the problem is thus not captured by the Anderson dimer.

3.3 Anderson molecule vs Hubbard dimer

Let us now compare the Anderson molecule and the Hubbard dimer. The non-interacting Green function for the Anderson molecule can be obtained directly from the non-interacting part of the Hamiltonian

$$\mathcal{G}_\sigma^{-1}(i\nu_n) = \begin{pmatrix} i\nu_n - \varepsilon_f + \mu & t_A \\ t_A & i\nu_n - \varepsilon_s + \mu \end{pmatrix}^{-1}.$$

By downfolding the s orbital we obtain

$$\mathcal{G}_{ff,\sigma}(i\nu_n) = \frac{1}{i\nu_n - (\varepsilon_f - \mu + \mathcal{F}(i\nu_n))},$$

where $\mathcal{F}(i\nu_n)$ is the non-interacting hybridization function for the Anderson molecule

$$\mathcal{F}(i\nu_n) = \frac{t_A^2}{i\nu_n - (\varepsilon_s - \mu)} = i\nu_n - \varepsilon_f + \mu - \mathcal{G}_{ff,\sigma}^{-1}(i\nu_n).$$

Using the Dyson equation, we can then write the interacting local Green function as

$$G_{ff,\sigma}(i\nu_n) = \frac{1}{i\nu_n - (\varepsilon_f - \mu + \mathcal{F}(i\nu_n) + \Sigma_{ff}(i\nu_n))}. \tag{13}$$

The impurity Green function (13) and the local Green function $G_{ii,\sigma}(i\nu_n)$ of the Hubbard dimer, Eq. (6), have a similar form. In view of this observation, it is legitimate to ask ourselves the following question: Can we reproduce some properties of the Hubbard dimer via an Anderson molecule in which $\varepsilon_f = \varepsilon_d$, while ε_s and t_A are free parameters? In the limit $U = 0$, indeed, setting $\varepsilon_s = \varepsilon_d$ and $t_A = t$ the two models are identical. For finite U, in general, they strongly differ. Let us request first that the occupation numbers is the same for the two models at half filling. This can be achieved with the choice

$$\varepsilon_s = \varepsilon_f + U/2.$$

For this value of ε_s, the eigenstates in the $N = 2$ electron sector are identical for the Hubbard dimer and the Anderson model. We can then in addition demand that at half-filling the gap is the same for the two models. This leads to the condition

$$\frac{1}{2}\sqrt{U^2 + 16t_A^2} = -2t + \sqrt{U^2 + 16t^2}$$

which for small t/U has the solution $t_A \sim \frac{\sqrt{3}}{4}U$. The message is that we could in principle use the Anderson molecule as an approximate version of the Hubbard dimer; choosing the parameters of the first ad hoc, we can reproduce some properties of the second, for example occupation number and gap. Could we go beyond that, and reproduce the full local Green function of the Hubbard dimer via an Anderson-like molecule? Comparing the local Green functions of the two models, we can see that it would be possible under, e.g., the following conditions

- the non-local part of the self-energy of the Hubbard dimer is negligible
- the local self-energy $\Sigma_l(i\nu_n)$ equals $\Sigma_{ff}(i\nu_n)$
- the hybridization function $\mathcal{F}(i\nu_n)$ equals $F(i\nu_n)$

As we have seen, for the Hubbard dimer the non-local part of the self-energy is finite and, in general, non-negligible; thus already the first condition is not fulfilled. For the lattice Hubbard model it can be shown, however, that diagrammatic perturbation theory greatly simplifies in the limit of infinite dimensions, and the self-energy becomes local [4,6]. This important conclusion is exploited in the DMFT approach.

4 DMFT and DFT+DMFT

4.1 Method

Although apparently simple, the Hubbard Hamiltonian (1) cannot be solved exactly except in special cases. For the Hubbard dimer defined via the Hamiltonian (4), we have seen that some properties can be reproduced via the even simpler Anderson molecule, Hamiltonian (12), provided that the parameters of the latter are chosen ad hoc. Can we do the same for the general Hubbard and Anderson model? This idea is at the core of dynamical mean-field theory. DMFT maps the correlated *lattice* problem described by the Hubbard model onto a correlated single-impurity problem [8, 4–6], e.g., an effective Anderson-like model. The latter can be solved exactly, differently than the original Hubbard model; to solve it we have to use numerical techniques, for example quantum Monte Carlo. The Anderson model is defined via either the hybridization function $\mathcal{F}(i\nu_n)$ or the bath Green function $\mathcal{G}(i\nu_n) = (i\nu_n - \varepsilon_d + \mu - \mathcal{F}(i\nu_n))^{-1}$. Solving it yields the impurity Green function $G(i\nu_n)$. From the Dyson equation we can calculate the impurity self-energy

$$\Sigma(i\nu_n) = \mathcal{G}^{-1}(i\nu_n) - G^{-1}(i\nu_n).$$

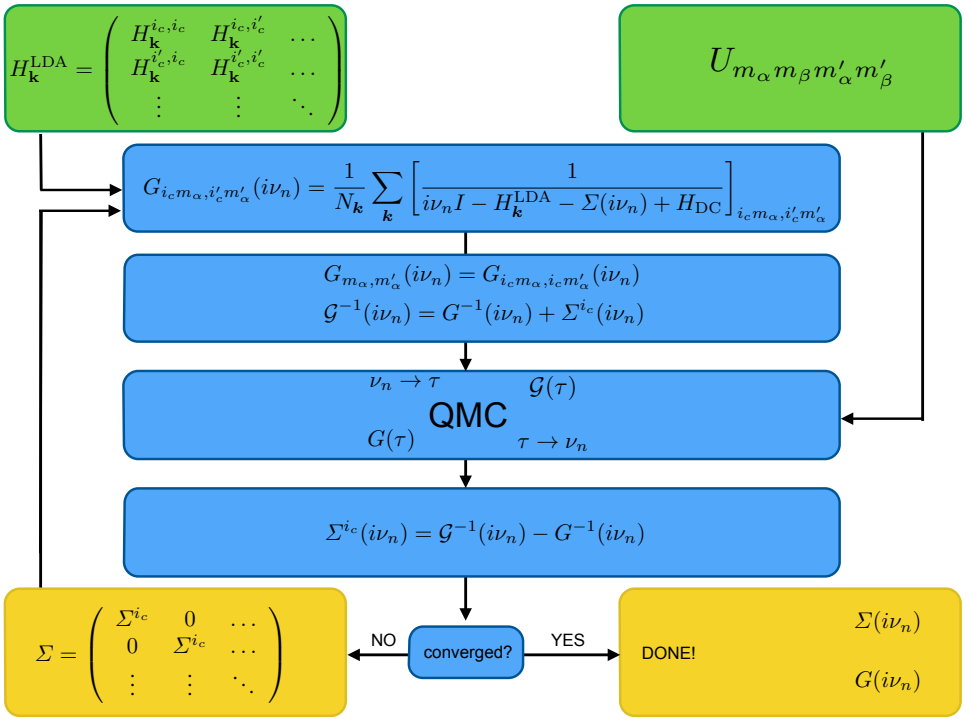

Fig. 7: *DFT+DMFT self-consistency loop. The DFT Hamiltonian is built in the basis of Bloch states obtained from localized Wannier functions, for example in the local-density approximation (LDA); this gives $H^{\mathrm{LDA}}_{\boldsymbol{k}}$. The set $\{i_c\}$ labels the equivalent correlated sites inside the unit cell. The local Green-function matrix is at first calculated using an initial guess for the self-energy matrix. The bath Green-function matrix is then obtained via the Dyson equation and used to construct an effective quantum-impurity model. The latter is solved via a quantum-impurity solver, here quantum Monte Carlo (QMC), yielding the impurity Green-function matrix. Through the Dyson equation the self-energy is then obtained, and the procedure is repeated till self-consistency is reached.*

Next, we assume that non-local contributions to the self-energy of the Hubbard model can be neglected, and that the local self-energy equals the impurity self-energy. Then, the local Green function is given by

$$G_{i_c,i_c}(i\nu_n) = \frac{1}{N_{\boldsymbol{k}}} \sum_{\boldsymbol{k}} \left[i\nu_n - \varepsilon_{\boldsymbol{k}} - \Sigma(i\nu_n) \right]^{-1} .$$

Here $N_{\boldsymbol{k}}$ is the number of $\boldsymbol{k}$ points. Self-consistency is reached when the impurity Green function $G(i\nu_n)$ equals the actual local Green function $G_{i_c,i_c}(i\nu_n)$

$$G_{i_c,i_c}(i\nu_n) = G(i\nu_n).$$

The main approximation adopted is that the self-energy of the Hubbard model is local; as already mentioned, it can be shown that the self-energy becomes indeed local in the infinite-coordination-number limit [4, 6]. The DMFT approach can be extended to material-specific multi-orbital Hamiltonians. In this case we replace

$$\varepsilon_{\boldsymbol{k}} \to H^0_{\boldsymbol{k}},$$

where $H^0_{\boldsymbol{k}}$ is the non-interacting Hamiltonian. Furthermore, the local Green function and self-energy become matrices in spin-orbital space. Typically, to build minimal material-specific models, we use density-functional theory, for example in the local-density approximation. First we construct a basis of localized Wannier functions that span the relevant bands and then use this basis to build material-specific Hubbard models. The combination of DMFT with density-functional theory, sketched above in short, defines the DFT+DMFT approach. The DMFT self-consistency loop is shown in Fig. 7, where it is assumed that quantum Monte Carlo (QMC) is used as the quantum-impurity solver. It has to be pointed out that the computational time needed to solve a multiband quantum-impurity models with QMC increases rapidly with the number of degrees of freedom. How rapidly depends on the specific QMC flavor used. Thus, in practice, only few correlated orbitals/sites can be treated fully with DMFT. Furthermore, increasing the number of degrees of freedom, eventually leads to the infamous sign problem. It is thus very important to properly build minimal material-specific models.

4.2 Model building in DFT+DMFT

In the Born-Oppenheimer approximation, the non-relativistic electronic Hamiltonian for an ideal crystal, $\hat{H}_e$, can be written as the sum of a one-electron $\hat{H}_0$ and an interaction part $\hat{H}_U$

$$\hat{H}_e = \hat{H}_0 + \hat{H}_U.$$

Let us assume that we have constructed a complete basis of Wannier functions $\psi_{in\sigma}(\boldsymbol{r})$. Then, in this basis, the one-electron term is given by

$$\hat{H}_0 = -\sum_{\sigma}\sum_{ii'}\sum_{nn'} t^{i,i'}_{n,n'} c^{\dagger}_{in\sigma} c_{i'n'\sigma},$$

where $c^{\dagger}_{in\sigma}$ ($c_{in\sigma}$) creates (destroys) an electron with spin σ in orbital n at site i. The on-site ($i = i'$) terms yield the crystal-field matrix while the $i \neq i'$ contributions are the hopping integrals. This part of the Hamiltonian describes the attraction between electrons and nuclei, the latter forming an ideal lattice. The electron-electron repulsion $\hat{H}_U$ is instead given by

$$\hat{H}_U = \frac{1}{2}\sum_{ii'jj'}\sum_{\sigma\sigma'}\sum_{nn'pp'} U^{iji'j'}_{np\,n'p'} c^{\dagger}_{in\sigma} c^{\dagger}_{jp\sigma'} c_{j'p'\sigma'} c_{i'n'\sigma}.$$

For a given system, *material-specific* Wannier functions can be obtained via DFT-based calculations [7, 8]. This immediately gives hopping integrals and crystal-field splittings

$$t^{i,i'}_{n,n'} = -\int d\mathbf{r}\, \overline{\psi_{in\sigma}}(\boldsymbol{r}) \left[-\frac{1}{2}\nabla^2 + v_{\rm R}(\boldsymbol{r})\right] \psi_{i'n'\sigma}(\boldsymbol{r}),$$

where $v_R(\boldsymbol{r})$ is the self-consistent DFT reference potential. The *bare* Coulomb integrals can be expressed in terms of Wannier functions as well

$$U^{iji'j'}_{np\,n'p'} = \int d\mathbf{r}_1 \int d\mathbf{r}_2\, \overline{\psi_{in\sigma}}(\mathbf{r}_1)\overline{\psi_{jp\sigma'}}(\mathbf{r}_2)\frac{1}{|\mathbf{r}_1 - \mathbf{r}_2|}\psi_{j'p'\sigma'}(\mathbf{r}_2)\psi_{i'n'\sigma}(\mathbf{r}_1).$$

Here we have to be careful, however. The DFT potential includes in $v_{\rm R}(\boldsymbol{r})$ also Coulomb effects, via the long-range Hartree term and the exchange-correlation contribution; if we use, e.g., LDA Wannier functions as one-electron basis, to avoid double counting we have to subtract from $\hat{H}_U$ the effects already included in the LDA. This means that we have to replace

$$\hat{H}_U \to \Delta\hat{H}_U = \hat{H}_U - \hat{H}_{\rm DC},$$

where $\hat{H}_{\rm DC}$ is the double-counting correction. Unfortunately we do not know which correlation effects are exactly included in the LDA, and therefore the exact expression of $\hat{H}_{\rm DC}$ is also unknown. The remarkable successes of the LDA suggest, however, that in many materials the LDA is overall a good approximation, and therefore, in those systems at least, the term $\Delta\hat{H}_U$ can be neglected. What about strongly-correlated materials? Even in correlated systems, most likely the LDA works rather well for the delocalized electrons or in describing the average or the long-range Coulomb effects. Thus one can think of separating the electrons into *uncorrelated* and *correlated*; only for the latter we do take the correction $\Delta\hat{H}_U$ into account explicitly, assuming furthermore that $\Delta\hat{H}_U$ is local or almost local [7]. Typically, correlated electrons are those that partially retain their atomic character, e.g., those that originate from localized d and f shells; for convenience here we assume that in a given system they stem from a single atomic shell l (e.g., d for transition-metal oxides or f for heavy-fermion systems) and label their states with the atomic quantum numbers l and $m = -l, \ldots, l$ of that shell. Thus

$$U^{iji'j'}_{np,n'p'} \sim \begin{cases} U^{l}{}_{m_\alpha m_\beta m'_\alpha m'_\beta} & iji'j' = iiii \quad npn'p' \in l \\ 0 & iji'j' \neq iiii \quad npn'p' \notin l \end{cases}$$

and $\Delta\hat{H}_U$ is replaced by $\Delta\hat{H}^l_U = \hat{H}^l_U - \hat{H}^l_{\rm DC}$, where $\hat{H}^l_{\rm DC}$ is, e.g., given by the static mean-field contribution of $\hat{H}^l_U$. There is a drawback in this procedure, however. By splitting electrons into correlated and uncorrelated we implicitly assume that the main effect of the latter is the renormalization or *screening* of parameters for the former, in particular of the Coulomb interaction. The calculation of screening effects remains, unfortunately, a challenge to date. Approximate schemes are the constrained LDA and the constrained random-phase approximation (RPA) methods [7, 8]. Nevertheless, we have now identified the general class of models for strongly-correlated systems, namely the generalized Hubbard model

$$\hat{H}_e = \hat{H}^{\rm LDA} + \hat{H}^l_U - \hat{H}^l_{\rm DC}. \tag{14}$$

It is often convenient to integrate out or downfold empty and occupied states and work directly with a set of Wannier functions spanning the correlated bands only. In this case we have

$$\hat{H}^{\rm LDA} = -\sum_{ii'}\sum_{\sigma}\sum_{m_\alpha m'_\alpha} t^{i,i'}_{m_\alpha,m'_\alpha} c^\dagger_{im_\alpha\sigma} c_{i'm'_\alpha\sigma} = \sum_{\boldsymbol{k}}\sum_{\sigma}\sum_{m_\alpha m'_\alpha} \left[H^{\rm LDA}_{\boldsymbol{k}}\right]_{m_\alpha,m'_\alpha} c^\dagger_{\boldsymbol{k}m_\alpha\sigma} c_{\boldsymbol{k}m'_\alpha\sigma},$$

where the right-hand side is rewritten using as a one-electron basis Bloch functions $\psi_{\boldsymbol{k}m_\alpha\sigma}$ constructed from the Wannier functions $\psi_{im_\alpha\sigma}$. The local *screened* Coulomb interaction is instead given by

$$\hat{H}^l_U = \frac{1}{2}\sum_{i}\sum_{\sigma\sigma'}\sum_{m_\alpha m'_\alpha}\sum_{m_\beta m'_\beta} U_{m_\alpha m_\beta m'_\alpha m'_\beta} c^\dagger_{im_\alpha\sigma} c^\dagger_{im_\beta\sigma'} c_{im'_\beta\sigma'} c_{im'_\alpha\sigma}.$$

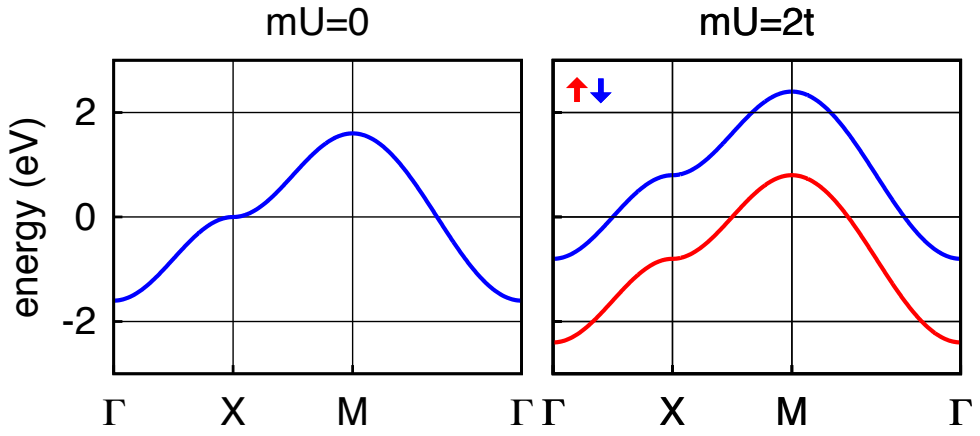

Fig. 8: *Ferromagnetism in Hartree-Fock. The chemical potential is taken as the energy zero.*

5 Metal-insulator transition

5.1 Hartree-Fock method

We have seen in section 2 the Hartree-Fock approximation for the Hubbard dimer. Here we want to extend it to the Hubbard model, and compare the description of the metal-insulator transition from Hartree-Fock to the one that emerges from DMFT. We assume that the system is at half-filling ($n = 1$) and exclude charge-disproportionation phenomena ($n_i = n$). Let us first consider the ferromagnetic HF solution. The HF approximation of the Coulomb term in the Hubbard model, as we have seen, consist in replacing the Coulomb term in the Hamiltonian with the expression given in Eq. (7). For the F solution we rewrite it as

$$\hat{H}_U^{\rm HF} = U \sum_i \left[-2m\hat{S}_z^i + m^2 + \frac{1}{4}n^2 \right],$$

were $m = (\bar{n}_{i\uparrow} - \bar{n}_{i\downarrow})/2 = m_+$. For the Hubbard model, it is convenient to Fourier transform the Hamiltonian to $\boldsymbol{k}$ space. We then adopt as one-electron basis the Bloch states

$$\Psi_{\boldsymbol{k}\sigma}(\boldsymbol{r}) = \frac{1}{\sqrt{N_s}} \sum_i e^{i\boldsymbol{k}\cdot\boldsymbol{T}_i}\, \Psi_{i\sigma}(\boldsymbol{r}),$$

where $\Psi_{i\sigma}(\boldsymbol{r})$ is a Wannier function with spin σ, $\boldsymbol{T}_i$ a lattice vector, and N_s the number of lattice sites. The term $\hat{H}_U^{\rm HF}$ depends on the spin operator $\hat{S}_z^i$, which can be written in $\boldsymbol{k}$ space as

$$\hat{S}_z^i = \frac{1}{N_{\boldsymbol{k}}} \sum_{\boldsymbol{kq}} e^{-i\boldsymbol{q}\cdot\boldsymbol{T}_i} \underbrace{\frac{1}{2} \sum_\sigma \sigma c^\dagger_{\boldsymbol{k}\sigma} c_{\boldsymbol{k}+\boldsymbol{q}\sigma}}_{S_z(\boldsymbol{k},\boldsymbol{k}+\boldsymbol{q})} = \frac{1}{N_{\boldsymbol{k}}} \sum_{\boldsymbol{kq}} e^{-i\boldsymbol{q}\cdot\boldsymbol{T}_i} \hat{S}_z(\boldsymbol{k},\boldsymbol{k}+\boldsymbol{q}).$$

The term $\hat{H}_U^{\rm HF}$ has the same periodicity as the lattice and does not couple states with different $\boldsymbol{k}$ vectors. Thus only $\hat{S}_z(\boldsymbol{0})$ contributes, and the Hamiltonian can be written as

$$\hat{H} = \sum_\sigma \sum_{\boldsymbol{k}} \varepsilon_{\boldsymbol{k}} \hat{n}_{\boldsymbol{k}\sigma} + \underbrace{U \sum_{\boldsymbol{k}} \left[-2m\, \hat{S}_z(\boldsymbol{k},\boldsymbol{k}) + m^2 + \frac{n^2}{4} \right]}_{\hat{H}_U^{\rm HF} = U\sum_i [-2m\hat{S}_z^i + m^2 + \frac{1}{4}n^2]},$$

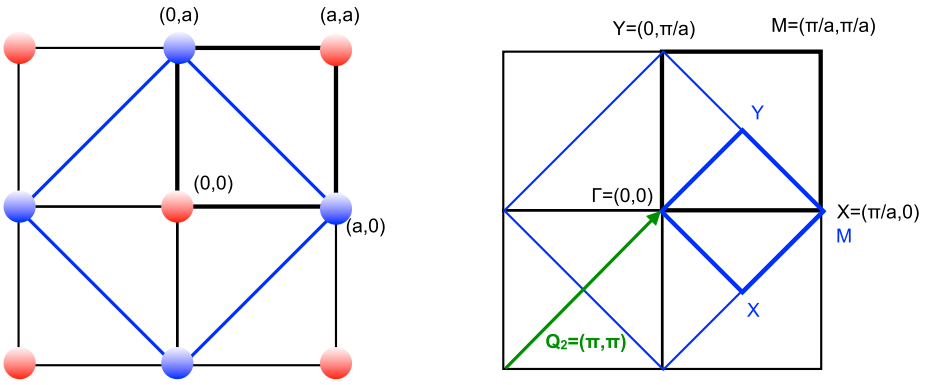

Fig. 9: *Doubling of the cell due to antiferromagnetic order and the corresponding folding of the Brillouin zone (BZ) for a two-dimensional hypercubic lattice. The antiferromagnetic* $\boldsymbol{Q}_2 = (\pi/a, \pi/a, 0)$ *vector is also shown.*

where for simplicity we set $\varepsilon_d = 0$. The HF correction splits the bands with opposite spin, leading to new one-electron eigenvalues, $\varepsilon_{\boldsymbol{k}\sigma} = \varepsilon_{\boldsymbol{k}} + \frac{1}{2}U - \sigma U m$. The separation between $\varepsilon_{\boldsymbol{k}\uparrow} - \mu$ and $\varepsilon_{\boldsymbol{k}\downarrow} - \mu$ is $2mU$, as can be seen in Fig. 8. The system remains metallic for U smaller than the bandwidth W. In the small-t/U limit and at half filling we can assume that the system is a ferromagnetic insulator and $m = 1/2$. The total energy of the ground state is then

$$E_{\mathrm{F}} = \frac{1}{N_{\boldsymbol{k}}} \sum_{\boldsymbol{k}} \left[\varepsilon_{\boldsymbol{k}\sigma} - \mu\right] = \frac{1}{N_{\boldsymbol{k}}} \sum_{\boldsymbol{k}} \left[\varepsilon_{\boldsymbol{k}} - \frac{1}{2}U\right] = -\frac{1}{2}U.$$

Let us now describe the same periodic lattice via a supercell which allows for a two-sublattice antiferromagnetic solution; this supercell is shown in Fig. 9. We rewrite the Bloch states of the original lattice as

$$\Psi_{\boldsymbol{k}\sigma}(\boldsymbol{r}) = \frac{1}{\sqrt{2}} \left[\Psi^A_{\boldsymbol{k}\sigma}(\boldsymbol{r}) + \Psi^B_{\boldsymbol{k}\sigma}(\boldsymbol{r})\right], \qquad \Psi^\alpha_{\boldsymbol{k}\sigma}(\boldsymbol{r}) = \frac{1}{\sqrt{N_{s_\alpha}}} \sum_{i_\alpha} e^{i\boldsymbol{T}^\alpha_i \cdot \boldsymbol{k}}\, \Psi_{i_\alpha\sigma}(\boldsymbol{r}).$$

Here A and B are the two sublattices with opposite spins and $\boldsymbol{T}^A_i$ and $\boldsymbol{T}^B_i$ are their lattice vectors; $\alpha = A, B$. We take as one-electron basis the two Bloch functions $\Psi_{\boldsymbol{k}\sigma}$ and $\Psi_{\boldsymbol{k}+\boldsymbol{Q}_2\sigma}$, where $\boldsymbol{Q}_2 = (\pi/a, \pi/a, 0)$ is the vector associated with the antiferromagnetic instability and the corresponding folding of the Brillouin zone, also shown in Fig. 9. Then, in HF approximation, setting $m_- = m$, the Coulomb interaction is given by

$$\hat{H}^{\mathrm{HF}}_U = \sum_{i\in A} \left[-2m\hat{S}^i_z + m^2 + \frac{n^2}{4}\right] + \sum_{i\in B} \left[+2m\hat{S}^i_z + m^2 + \frac{n^2}{4}\right].$$

This interaction couples Bloch states with $\boldsymbol{k}$ vectors made equivalent by the folding of the Brillouin zone. Thus the HF Hamiltonian takes the form

$$\hat{H} = \sum_{\boldsymbol{k}}\sum_{\sigma} \varepsilon_{\boldsymbol{k}} \hat{n}_{\boldsymbol{k}\sigma} + \sum_{\boldsymbol{k}}\sum_{\sigma} \varepsilon_{\boldsymbol{k}+\boldsymbol{Q}_2} \hat{n}_{\boldsymbol{k}+\boldsymbol{Q}_2\sigma} + \underbrace{U \sum_{\boldsymbol{k}} \left[-2m\, \hat{S}_z(\boldsymbol{k}, \boldsymbol{k}+\boldsymbol{Q}_2) + 2m^2 + \frac{n^2}{2}\right]}_{\text{static mean-field correction } \hat{H}^{\mathrm{HF}}_U}.$$

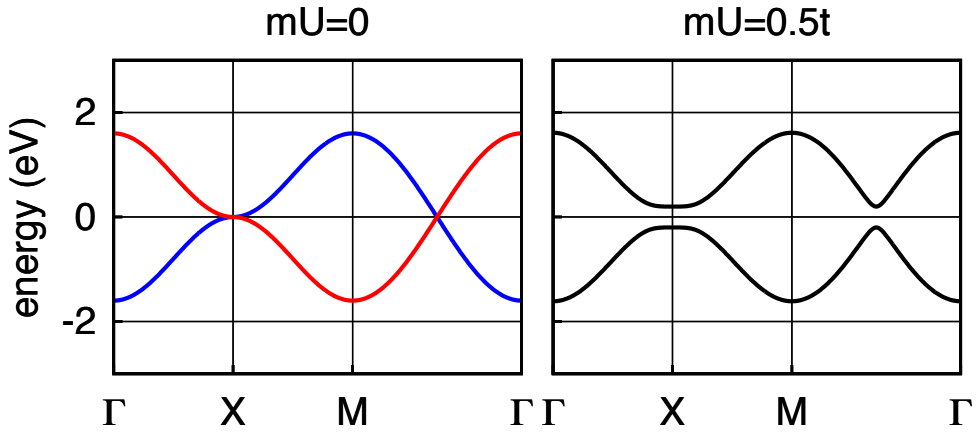

Fig. 10: *Antiferromagnetism in Hartree-Fock. The chemical potential is taken as the energy zero. Blue:* $\varepsilon_{\boldsymbol{k}}$*. Red:* $\varepsilon_{\boldsymbol{k}+\boldsymbol{Q}_2} = -\varepsilon_{\boldsymbol{k}}$*. The high-symmetry lines are those of the large BZ in Fig. 9.*

The sum over $\boldsymbol{k}$ is restricted to the Brillouin zone of the antiferromagnetic lattice. We find the two-fold degenerate eigenvalues

$$\varepsilon_{\boldsymbol{k}\pm} - \mu = \frac{1}{2}(\varepsilon_{\boldsymbol{k}} + \varepsilon_{\boldsymbol{k}+\boldsymbol{Q}_2}) \pm \frac{1}{2}\sqrt{(\varepsilon_{\boldsymbol{k}} - \varepsilon_{\boldsymbol{k}+\boldsymbol{Q}_2})^2 + 4(mU)^2}. \tag{15}$$

A gap opens where the bands $\varepsilon_{\boldsymbol{k}}$ and $\varepsilon_{\boldsymbol{k}+\boldsymbol{Q}_2}$ cross, e.g., at the X point of the original Brillouin zone (Fig. 10). At half filling and for $mU = 0$ the Fermi level crosses the bands at the X point; thus the system is an insulator for any finite value of mU. In the small-t/U limit we can assume that $m = 1/2$ and expand the eigenvalues in powers of $\varepsilon_{\boldsymbol{k}}/U$. For the occupied states we find

$$\varepsilon_{\boldsymbol{k}-} - \mu \sim -\frac{1}{2}U - \frac{\varepsilon_{\boldsymbol{k}}^2}{U} = -\frac{1}{2}U - \frac{4t^2}{U}\left(\frac{\varepsilon_{\boldsymbol{k}}}{2t}\right)^2.$$

The ground-state total energy for the antiferromagnetic supercell is then $2E_{\rm AF}$ with

$$E_{\rm AF} = -\frac{1}{2}U - \frac{4t^2}{U}\frac{1}{N_{\boldsymbol{k}}}\sum_{\boldsymbol{k}}\left(\frac{\varepsilon_{\boldsymbol{k}}}{2t}\right)^2 \sim -\frac{1}{2}U - \frac{4t^2}{U}$$

so that the energy difference per pair of spins between ferro- and antiferro-magnetic state is

$$\Delta E^{\rm HF} = E^{\rm HF}_{\uparrow\uparrow} - E^{\rm HF}_{\uparrow\downarrow} = \frac{2}{n_{\langle ii'\rangle}}\left[E_{\rm F} - E_{\rm AF}\right] \sim \frac{1}{2}\frac{4t^2}{U} \sim \frac{1}{2}\Gamma, \tag{16}$$

which is similar to the result obtained from the Hubbard model in many-body second order perturbation theory, Eq. (3). We notice here the same problems that we already observed for the Hubbard dimer. Despite the similarity with the actual solution, the spectrum of the Hartree-Fock Hamiltonian has very little to do with the spectrum of the Hubbard Hamiltonian at half filling. If we restrict ourselves to the AF solution, the first excited state in HF is at an energy $\propto U$ rather than $\propto \Gamma$; thus, we cannot use a single HF calculation to understand the magnetic excitation spectrum of a given system. It is more meaningful to use HF to compare the total energy of different states and determine in this way, within HF, the ground state. Even in this

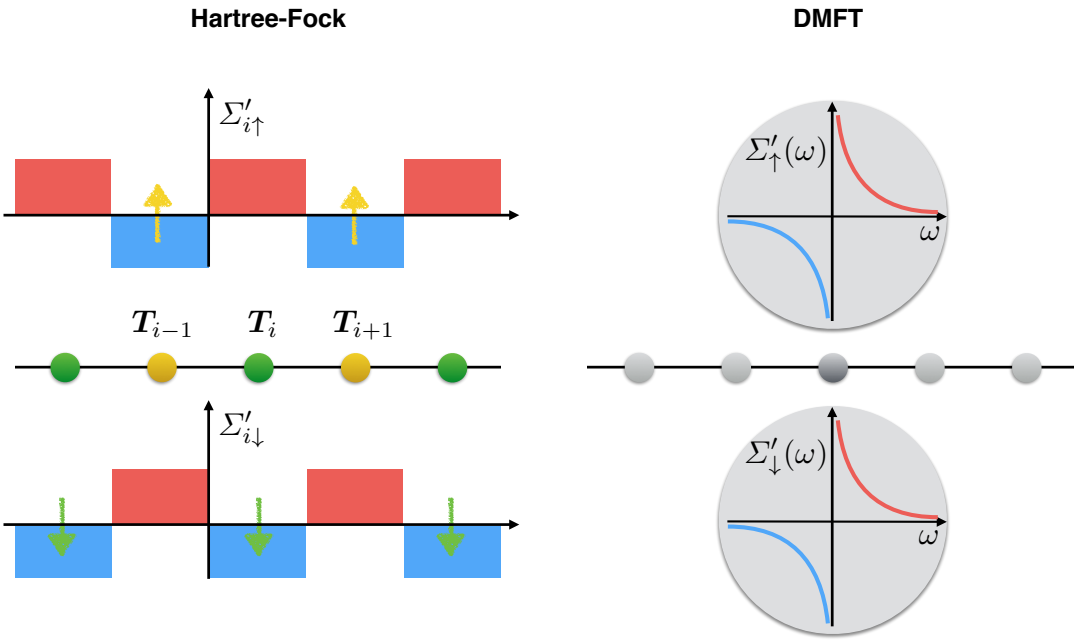

Fig. 11: *Idealized correlated crystal, schematically represented by a half-filled single-band Hubbard chain. Sketch of the real-part of the self-energy in the insulating phase, as described by Hartree-Fock (left-hand side) and DMFT (right-hand side). In HF the self-energy is a spin- and site-dependent potential (Slater insulator). In DMFT it is spin- and site-independent; it is, however, dynamical and its real part diverges at zero frequency (Mott insulator). The imaginary part of the self-energy is always zero in Hartree-Fock (i.e., quasiparticles have infinite lifetimes).*

case, however, as we have seen for the Hubbard dimer, HF suffers from spin contamination, i.e., singlet states and $S_z = 0$ triplet states mix. The energy difference per bond $E^{\mathrm{HF}}_{\uparrow\uparrow} - E^{\mathrm{HF}}_{\uparrow\downarrow}$ in Eq. (16) only resembles the exact result; the exact energy difference between triplet and singlet state in the Hubbard dimer is a factor of two larger

$$\Delta E = E_{S=1} - E_{S=0} = \Gamma.$$

Thus, overall, HF is not the ideal approach to determine the onset of magnetic phase transitions. The major problem of the HF approximation is, however, the description of the metal-insulator transition. In HF the metal-insulator transition is, as we have seen, intimately related to long-range magnetic order, i.e., it is a Slater rather than a Mott transition. If we write the HF correction in the form of a self-energy, the latter is a real, static but spin- and site-dependent potential. More specifically, in the AF case at half filling we have for two neighboring sites i and j

$$\Sigma^{\mathrm{HF}}_{i\sigma}(\omega) = U\left[\frac{1}{2} + m\right], \quad \Sigma^{\mathrm{HF}}_{j\sigma}(\omega) = U\left[\frac{1}{2} - m\right].$$

This spatial structure of the self-energy is what opens the gap shown in Fig. 10. For $m = 0$ the self-energy is a mere energy shift – the same for all sites and spins – and does not change the band structure or the properties of the system, which is then a conventional metal.

5.2 HF vs DMFT

The main difference between DMFT and Hartree-Fock is that in DMFT the self-energy is frequency dependent but local (i.e., site- or $\boldsymbol{k}$-independent), while in HF is static but site dependent. Let us discuss the DMFT description of the metal-insulator transition. The poles of the Green function, i.e., the solutions of the equation

$$\omega - \varepsilon_{\boldsymbol{k}} - \Sigma'(\omega) = 0\,,$$

where $\Sigma'(\omega)$ is the real part of the self-energy, yield the excitations of our system. For small U, in the Fermi liquid regime, the Green function has a pole at zero frequency. Around it, the DMFT self-energy for the Hubbard model has, on the real axis, the following form

$$\Sigma(\omega) \sim \frac{1}{2}\,U + \left(1 - \frac{1}{Z}\right)\omega - \frac{i}{2\tau^{\rm QP}},$$

where the positive dimensionless number Z yields the mass enhancement,

$$\frac{m^*}{m} \sim \frac{1}{Z} = 1 - \left.\frac{d\Sigma'(\omega)}{d\omega}\right|_{\omega\to 0}$$

and the positive parameter $\tau^{\rm QP}$ is the quasiparticles lifetime

$$\frac{1}{\tau^{\rm QP}} \sim -2Z\Sigma''(0) \propto (\pi k_B T)^2 + \omega^2.$$

At higher frequency the self-energy yields additional poles corresponding to the Hubbard bands. For large U, in the insulating regime, the central quasiparticle peak disappears, and only the Hubbard bands remain. The self-energy has approximately the form

$$\Sigma(\omega) \sim \frac{rU^2}{4}\left[\frac{1}{\omega} - i\pi\delta(\omega) - i f_U(\omega)\right],$$

where $f_U(\omega)$ is a positive function that is zero inside the gap and r is a model-specific renormalization factor. Hence, the real-part of the self-energy diverges at zero frequency, and there are no well defined low-energy quasiparticles. Furthermore, since we are assuming that the system is paramagnetic, the self-energy and the Green function are independent of spin. Thus, in DMFT the gap opens via the divergence at zero frequency in the real-part of the self-energy; this happens already in a single-site paramagnetic calculation, i.e., we do not have to assume any long-range magnetic order. What is then the relation between HF and DMFT? As can be understood from the discussion above, HF is not the large-U limit of DMFT. Since the HF self-energy is frequency independent, HF quasi-particles have infinite lifetime and bare masses ($Z = 1$ and $m^* = m$). These quasi-particles exist both in the metallic and in the insulating regime. It can be shown, however, that the DMFT self-energy reduces to the HF self-energy in the large-frequency limit. The main differences between HF and DMFT are pictorially shown in Fig. 11 for an idealized one-dimensional crystal.

5.3 DFT+*U* vs DFT+DMFT

The DFT+*U* method was the first systematic attempt to construct and solve *ab-initio* many-body Hamiltonians [3]. The model building part is very similar in DFT+DMFT and DFT+U, except that the latter was developed already fully embedded in density-functional theory, and therefore it might appear different at a first glance. In DFT+U the Coulomb interaction is treated in static mean-field theory, and therefore, as we can now understand, true many-body effects, such as the frequency dependence of the self-energy, are lost. Let us first assume that Hamiltonian (14) has the simplified form

$$\hat{H}^{\rm LDA} + \hat{U}^l - \hat{H}^l_{\rm DC} = \hat{H}^{\rm LDA} + \frac{1}{2}U\sum_i \sum_{m\sigma\neq m'\sigma'} \hat{n}_{im\sigma}\hat{n}_{im'\sigma'} - \underbrace{\frac{1}{2}U\sum_i \sum_{m\sigma\neq m'\sigma'} \langle\hat{n}_{im\sigma}\rangle\langle\hat{n}_{im'\sigma'}\rangle}_{\text{mean-field energy, } \mathrm{E_{MF}}}.$$

Next, we treat the Coulomb interaction in static mean-field via the HF decoupling; we approximate the mean-field energy in the expression above by the Hartree energy, taking for convenience as the energy zero the atomic chemical potential $\mu_{\rm AT} = U/2$

$$E_{MF} = E_H - \mu_{\rm AT} N^l = \frac{1}{2}UN^lN^l - \frac{1}{2}UN^l.$$

Here $N^l = \sum_{m\sigma}\langle\hat{n}_{im\sigma}\rangle$ is the number of heavy electrons per site. The mean-field Hamiltonian takes then the form

$$\hat{H} = \hat{H}^{\rm LDA} + \sum_{im\sigma} t^\sigma_m \hat{n}_{im\sigma}, \quad \text{with} \quad t^\sigma_m = U\left(\frac{1}{2} - \langle\hat{n}_{im\sigma}\rangle\right).$$

The levels of the correlated electrons are shifted by $-U/2$ if occupied and by $U/2$ if empty, like in the atomic limit of the half-filled Hubbard model. A total energy functional which shifts the LDA orbital energies in this way is

$$E_{\rm LDA+U}[n] = E_{\rm LDA}[n] + \sum_i \left[\frac{1}{2}U \sum_{m\sigma\neq m'\sigma'} \langle\hat{n}_{im\sigma}\rangle\langle\hat{n}_{im'\sigma'}\rangle - E_{\rm DC}\right],$$

where the double-counting term is

$$E_{\rm DC} = \frac{1}{2}UN^l(N^l - 1)$$

and $E_{LDA}[n]$ is the total energy obtained using the spin-polarized version of the local-density approximation for the exchange-correlation functional. Indeed

$$\varepsilon^{\rm LDA+U}_{im\sigma} = \frac{\partial E_{\rm LDA+U}}{\partial\langle\hat{n}_{im\sigma}\rangle} = \varepsilon^{\rm LDA}_{im\sigma} + U\left(\frac{1}{2} - \langle\hat{n}_{im\sigma}\rangle\right) = \varepsilon^{\rm LDA}_{im\sigma} + t^\sigma_m.$$

More generally, the DFT+*U* functional is given by a form of the type

$$E_{\rm LDA+U}[n] = E_{\rm LDA}[n] + \frac{1}{2}\sum_{i\sigma} \sum_{mm'm''m'''} U_{mm''m'm'''} \langle\hat{n}^\sigma_{imm'}\rangle\langle\hat{n}^{\text{-}\sigma}_{im''m'''}\rangle$$

$$+ \frac{1}{2}\sum_{i\sigma} \sum_{mm'm''m'''} \left[U_{mm''m'm'''} - U_{mm''m'''m'}\right] \langle\hat{n}^\sigma_{imm'}\rangle\langle\hat{n}^\sigma_{im''m'''}\rangle - E_{\rm DC},$$

where $\langle \hat{n}^\sigma_{imm'} \rangle = \langle c^\dagger_{im\sigma} c_{im'\sigma} \rangle$ is the density matrix, and $\langle \hat{n}_{im\sigma} \rangle = \langle \hat{n}^\sigma_{imm} \rangle$. One of the most common recipes for the double-counting correction is the fully-localized limit

$$E_{\rm DC} = \frac{1}{2} U_{\rm avg} N^l (N^l - 1) - \frac{1}{2} J_{\rm avg} \sum_\sigma N^l_\sigma (N^l_\sigma - 1),$$

where

$$U_{\rm avg} = \frac{1}{(2l+1)^2} \sum_{m,m'} U_{mm'mm'},$$

$$U_{\rm avg} - J_{\rm avg} = \frac{1}{2l(2l+1)} \sum_{m,m'} (U_{mm'mm'} - U_{mm'm'm}).$$

The corresponding one-electron DFT+*U* Hamiltonian is

$$\hat{H} = \hat{H}^{\rm LDA} + \sum_{imm'\sigma} t^\sigma_{mm'} c^\dagger_{im\sigma} c_{im'\sigma}, \tag{17}$$

where

$$t^\sigma_{mm'} = \sum_{i\sigma} \sum_{m''m'''} U_{mm''m'm'''} \langle \hat{n}^{-\sigma}_{im''m'''} \rangle + [U_{mm''m'm'''} - U_{mm''m'''m'}] \langle \hat{n}^\sigma_{im''m'''} \rangle$$

$$- \left[U_{\rm avg} \left(N^l - \frac{1}{2} \right) - J_{\rm avg} \left(N^l_\sigma - \frac{1}{2} \right) \right] \delta_{m,m'}.$$

The second common recipe for the double-counting correction is the around mean-field limit; here the double-counting energy is the mean-field energy for equally occupied orbitals

$$E_{\rm DC} = U_{\rm avg} N^l_\uparrow N^l_\downarrow + \frac{2l}{2(2l+1)} (U_{\rm avg} - J_{\rm avg}) \left(N^2_\uparrow + N^2_\downarrow \right).$$

The corresponding one-electron LDA+*U* Hamiltonian is (17) with

$$t^\sigma_{mm'} = \sum_{i\sigma} \sum_{m''m'''} U_{mm''m'm'''} \langle \hat{n}^{-\sigma}_{im''m'''} \rangle + [U_{mm''m'm'''} - U_{mm''m'''m'}] \langle \hat{n}^\sigma_{im''m'''} \rangle$$

$$- \left[U_{\rm avg} \left(N^l - n_\sigma \right) - J_{\rm avg} \left(N^l_\sigma - n_\sigma \right) \right] \delta_{m,m'},$$

where $n_\sigma = N_l/(2(2l+1))$ is the average occupation per spin. In DFT+DMFT the same recipes are used for the double-counting correction; this is reasonable because the source of double-counting is the same in the two methods. In DFT+*U*, differently than in static mean-field for model Hamiltonians, $\hat{H}^{\rm LDA}$ is obtained self-consistently. The DFT+*U* correction in (17) modifies the occupations of the correlated sector with respect to LDA. If we assume that LDA describes uncorrelated electrons sufficiently well, the readjustments in the uncorrelated sector can be calculated by making the total charge density and the reference potential consistent within the LDA (*charge self-consistency*), however with the constraint given by (17). Using

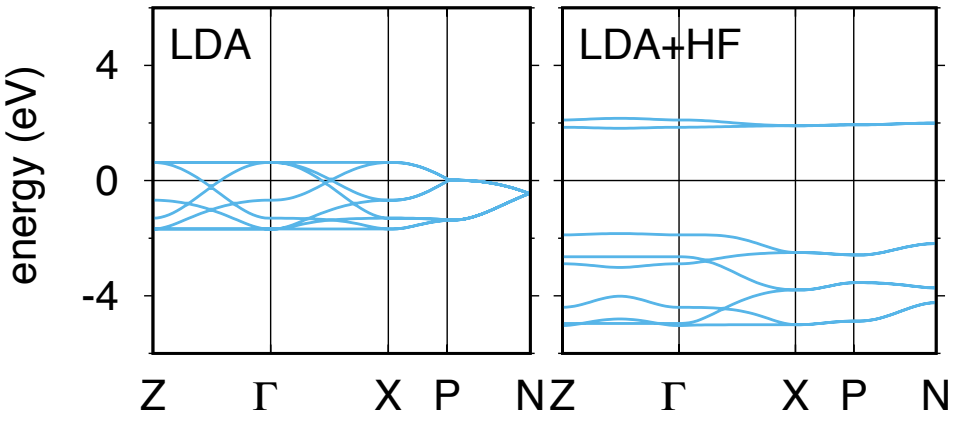

Fig. 12: *Left: LDA e_g band structure of cubic $KCuF_3$ calculated using the experimental magnetic unit cell with four formula units. Right: Static mean-field band structure, calculated for the experimental orbital and spin order. Parameters: $U = 7\ eV$ and $J = 0.9\ eV$.*

the same procedure, charge self-consistency can of course also be achieved in DFT+DMFT calculations. A difficulty is, however, the basis. DFT+*U* calculations are usually not performed in a Wannier basis. They are typically based on the identification of an *atomic sphere*, a region of space in which correlated electrons are well described by atomic-like orbitals; the DFT+*U* correction is determined through projections onto such atomic orbitals. Thus DFT+*U* results are essentially dependent on the choice of the set of correlated electrons and their atomic spheres. If the correlated electrons are well localized, however, they retain to a good extent their atomic character in a solid. Thus, within reasonable sphere choices, the dependence on the sphere size is less crucial than could be expected. Still, from a theoretical point of view, there is an inconsistency in this procedure. Orbitals defined only within the atomic spheres do not form a complete basis (even for the correlated sector), and thus they do not really yield a many-body Hamiltonian of the form (14). One of the successes of DFT+*U* is that it describes well the magnetic ground-state of Mott insulators. The method has however all defects of the HF approximation; it opens a gap by making long-range order, eigenvalues are real, and quasi-particles have an infinite lifetime. One further example of the failure of DFT+U is the description of the super-exchange driven orbital-order transition. Let us consider the insulating perovskite $KCuF_3$ as representative material. Instead of the full DFT+*U* calculation, for simplicity we discuss the calculation for the e_g-band Hubbard model describing the low-energy states and do not perform any charge self-consistency. For this Hamiltonian the double-counting correction is a mere shift of the chemical potential and can be neglected. The model has the form

$$\hat{H} = -\sum_{m,m',i,i',\sigma} t^{i,i'}_{mm'} c^{\dagger}_{im\sigma} c_{im'\sigma} + U \sum_{i\ m} \hat{n}_{im\uparrow}\hat{n}_{im\downarrow} + \frac{1}{2} \sum_{\substack{i\sigma\sigma' \\ m\neq m'}} (U - 2J - J\delta_{\sigma,\sigma'}) \hat{n}_{im\sigma}\hat{n}_{im'\sigma'}$$

$$-J \sum_{i\ m\neq m'} \left[c^{\dagger}_{im\uparrow} c^{\dagger}_{im\downarrow} c_{im'\uparrow} c_{im'\downarrow} + c^{\dagger}_{im\uparrow} c_{im\downarrow} c^{\dagger}_{im'\downarrow} c_{im'\uparrow} \right]$$

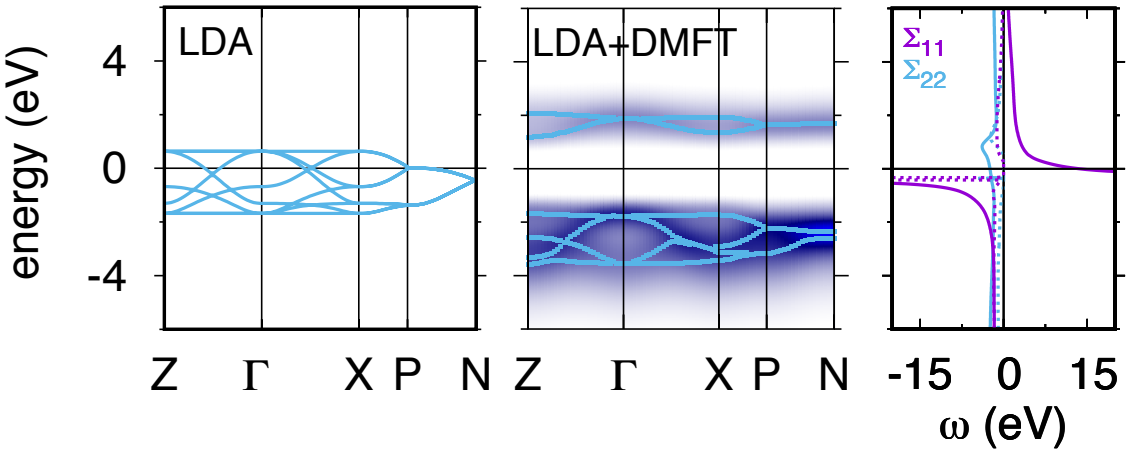

Fig. 13: *Left: LDA band structure of $KCuF_3$, e_g bands. Center: corresponding LDA+DMFT correlated band structure in the orbitally-ordered phase [16]. Dots: poles of the Green function. Right: Self-energy matrix in the basis of the natural orbitals. Full lines: real part. Dotted lines: imaginary part. Parameters: $U = 7$ eV, $J = 0.9$ eV.*

where $m, m' = 3z^2 - r^2, x^2 - y^2$. The last two terms describe the pair-hopping ($U_{mmm'm'} = J_{m,m'}$ for real harmonics, while for spherical harmonics $U_{mmm'm'} = 0$) and spin-flip processes. The question to be answered is: Can orbital order arise spontaneously for the ideal perovskite cubic structure in which the e_g orbitals are degenerate? $KCuF_3$ is, in nature, an insulator, but in LDA it turns out to be metallic and exhibits no orbital order. This can be seen in Fig. 12. In DFT+U, in order to open the gap, we have first to double the cell. The gap opens only in the presence of both spin and orbital order. This means that there is no phase in which the system is non-magnetic but has a gap and exhibits orbital order. We could paraphrase this result by saying that,[1] in DFT+U

$$T_N = T_{OO} = T_{MI}$$

where T_N, T_{OO}, T_{MI} are the critical temperature at which the magnetic, orbital and metal-insulator transition occur. For the magnetic orbitally ordered phase, the resulting electronic structure is shown in Fig. 12. Let us now discuss the solution of the same problem with DFT+DMFT. With this approach we obtain an insulating orbitally ordered solution even in the absence of long-range magnetic order. DMFT describes the correct sequence of phenomena

$$T_N < T_{OO} < T_{MI}.$$

In Fig. 13 we show the DFT+DMFT *paramagnetic* e_g correlated band structure of $KCuF_3$ in the orbitally ordered phase. We can compare these bands with the static mean-field *antiferromagnetic* band structure in Fig. 12. The DFT+DMFT band gap is significantly smaller. The imaginary part of the self-energy, which is zero in static mean-field theory, makes the Hubbard bands partly incoherent. The real part of the self-energy of the half-filled orbital (Fig. 13), which in static mean-field theory does not depend on ω, diverges at low frequencies.

[1] This, of course, oversimplifies the discussion, since DFT+U is a $T = 0$ method.

6 Conclusions

In this lecture we have discussed two methods that can be used for describing the metal-insulator transition in Hubbard-like models. The first method is the Hartree-Fock approach. Here the Coulomb interaction part of the Hubbard Hamiltonian is treated at the static mean-field level. The occupation matrix is determined self-consistently. The Hartree-Fock self-energy is equivalent to a site-, orbital-, and spin-dependent potential. The metal-insulator transition occurs via an enlargement of the unit cell and a lowering of the symmetry. In this approach, all states have infinite lifetime and the masses of electrons are not renormalized. This is a Slater-type transition. The Hartree-Fock method is the basis of the DFT+U approach. Numerically, DFT+U calculations are as fast as standard DFT calculations. Furthermore, in DFT+U, the Hartree-Fock correction is embedded in the DFT formalism via a modification of the total-energy functional. One drawback is that typically the correction is for orbitals defined within an atomic sphere, and not Wannier function. This means that, strictly speaking, we could not use them alone to directly construct generalized Hubbard models. The second approach examined in this lecture is DMFT, dynamical mean-field theory. In DMFT the Hubbard model is mapped onto a quantum-impurity model, for example the Anderson Hamiltonian. The latter is solved exactly and yields the impurity self-energy. The hybridization function of the Anderson Hamiltonian is determined self-consistently, requiring the local Green function equals the impurity Green function. The central approximation is that the self-energy of the Hubbard model is assumed to be local. This approximation becomes progressively better with increasing coordination number; in infinite dimensions, indeed, the self-energy is local. In DMFT the metal-insulator transition has a very different nature than in Hartree-Fock. It occurs already above the magnetic transition and it happens via a divergence of the low-frequency self-energy. Switching on the Coulomb interaction leads at first to the formation of heavy quasi-particles with renormalized masses and finite life-times. Eventually, when U is above a critical value, the self-energy and the masses diverge, and the spectral function exhibits a gap. The metal-insulator transition described via DMFT is of Mott type. In DMFT we neglect the momentum-dependence of the self-energy. As we have seen in the case of the Hubbard dimer, such effects can be important; in particular they become important in low dimensions. Straightforward extensions of DMFT to include some non-local effects are cluster approaches, in real and $\mathbf{k}$ space. The bottleneck of DMFT is, however, the quantum impurity solver, typically quantum Monte Carlo. The computational time can increase very rapidly with the number of orbitals and sites, and eventually the infamous sign problem appears. The model and the cluster size has thus to be carefully chosen. The DMFT approach can be used also for realistic Hamiltonians built via density-functional theory. This is the DFT+DMFT approach. In both DFT+U and DMFT+U, a double-counting correction has to be subtracted, since part of the Coulomb effects are already included in the DFT functional, for example the LDA.

References

[1] K.F. Sundman, Acta Mathematica **36**, 105 (1912)

[2] F. Diacu, The Mathematical Intelligencer **18**, 66 (1996)

[3] A.I. Lichtenstein, M.I. Katsnelson, and V.A. Gubanov, J. Phys. F **14**, L125;
Solid State Commun. **54**, 327 (1985);
A.I. Lichtenstein, M.I. Katsnelson, V.P. Antropov, and V.A. Gubanov,
J. Magn. Magn. Mater. **67**, 65 (1987);
M.I. Katsnelson and A.I. Lichtenstein, Phys. Rev. B **61**, 8906 (2000)

[4] W. Metzner and D. Vollhardt, Phys. Rev. Lett. **62**, 324 (1989);
A. Georges and G. Kotliar, Phys. Rev. B **45**, 6479 (1992)

[5] M. Jarrell, Phys. Rev. Lett. **69**, 168 (1992)

[6] E. Müller-Hartmann, Z. Phys. B **74**, 507 (1989);
Z. Phys. B **76**, 211 (1989); Int. J. Mod. Phys. B **3**, 2169 (1989)

[7] E. Pavarini, E. Koch, A. Lichtenstein, D. Vollhardt:
The LDA+DMFT approach to strongly-correlated materials,
Reihe Modeling and Simulation, Vol. 1 (Forschungszentrum Jülich, 2011)
`http://www.cond-mat.de/events/correl11`

[8] E. Pavarini, E. Koch, A. Lichtenstein, D. Vollhardt: *DMFT at 25: Infinite Dimensions*,
Reihe Modeling and Simulation, Vol. 4 (Forschungszentrum Jülich, 2014)
`http://www.cond-mat.de/events/correl14`

[9] A. Lagendijk, B. van Tiggelen, and D.S. Wiersma, Physics Today **62**, 24 (2009)

[10] J.R. Schrieffer and P.A. Wolff, Phys. Rev. **149**, 491 (1966);
A.H. MacDonald, S.M. Girvin and D. Yoshioka, Phys. Rev. B **37**, 9753 (1988)

[11] L. Cano-Cortés, A. Dolfen, J. Merino, J. Behler, B. Delley, K. Reuter and E. Koch,
Eur. Phys. J. B **56**, 173 (2007)

[12] E. Pavarini, I. Dasgupta, T. Saha-Dasgupta, O. Jepsen and O.K. Andersen,
Phys. Rev. Lett. **87**, 047003 (2001)

[13] P.W. Anderson, J. Phys. C: Solid State Phys. **3**, 2436 (1970)

[14] K. Wilson, Rev. Mod. Phys. **47**, 773 (1975)

[15] P. Nozières, J. Low. Temp. Phys. **17**, 31 (1974)

[16] E. Pavarini, E. Koch, A.I. Lichtenstein, Phys. Rev. Lett. **101**, 266405 (2008)